Journal of Water Process Engineering 70 (2025) 106993

Contents lists available at ScienceDirect

Journal of Water Process Engineering

journal homepage: www.elsevier.com/locate/jwpe

Recent advancements in smart materials for the removal of organic, inorganic and microbial pollutants in water treatment: A review

Soon Wah Goh [a], Qi Hwa Ng [a,b,*], Siti Kartini Enche Ab Rahim [a,b], Siew Chun Low [c], Peng Yong Hoo [a,b], Ryan Yow Zhong Yeo [d], Thiam Leng Chew [e,f], Zeinab Abbas Jawad [g]

[a] Faculty of Chemical Engineering & Technology, Universiti Malaysia Perlis (UniMAP), 02600 Arau, Perlis, Malaysia
[b] Centre of Excellence for Frontier Materials Research (CFMR), Universiti Malaysia Perlis (UniMAP), 02600 Arau, Perlis, Malaysia
[c] School of Chemical Engineering, Engineering Campus, Universiti Sains Malaysia, 14300 Nibong Tebal, Pulau Pinang, Malaysia
[d] Fuel Cell Institute, Universiti Kebangsaan Malaysia, 43600 Bangi, Selangor, Malaysia
[e] Department of Chemical Engineering, Faculty of Engineering, Universiti Teknologi PETRONAS, 32610 Seri Iskandar, Perak, Malaysia
[f] Centre of Carbon Capture, Utilization and Storage (CCCUS), Institute of Sustainable Energy & Resources (ISER), Universiti Teknologi PETRONAS, 32610 Seri Iskandar, Perak, Malaysia
[g] Department of Chemical Engineering, College of Engineering, Qatar University, P. O. Box: 2713, Doha, Qatar

ARTICLE INFO

Editor: Laura Bulgariu

Keywords:
Smart materials
Single-stimulus-responsive
Multi-stimuli-responsive
Organic, inorganic, and microbial pollutants
Water treatment

ABSTRACT

As the expeditious urban and industrial expansion, a substantial portion of wastewater is produced annually, posing a significant threat to environmental contamination and dwindling the availability of clean water resources. Water contaminants are generally categorized into organic, inorganic, and microbial pollutants. This escalating water pollution crisis has initiated the research community to innovate novel, effective and economical cost methods for water treatment applications. Among the approaches, adsorption has been marked by its importance in water treatment. Recent advancements in the field have focused on developing smart adsorbent materials capable of modifying their physicochemical properties in response to various external stimuli (light and magnetic field) and internal stimuli (thermal and pH fluctuation). The exploration of smart materials has captivated the interest of researchers worldwide and opened up exciting avenue for more efficient water treatment outcomes towards removing different types of pollutants. Notably, these smart materials demonstrate high pollutant uptake and release efficacy when responding to specific stimuli changes, ensuring efficient removal of contaminants and exerting self-cleaning properties. Such materials offer an environmentally benign advantage by eliminating the need for toxic organic solvents during regeneration. The review compiles and highlights the characteristics and performance of several stimuli-responsive smart materials, including thermal, light, magnetic and pH regarding organic, inorganic and microbial pollutants removal efficiencies. A particular focus is given to multi-stimuli responsive materials in environmental applications that represent the modern era and transformation of water treatment methodologies, followed by a discussion on the challenges and prospects of this particular research area.

1. Introduction

In the past couple of decades, rapid urbanization, expanding industrialization, increasing agricultural production needs, climate change and water-related pollution have brought tremendous pressure on clean water resources [1–3]. According to the United Nations World Water Development report, over 2 billion people reside in countries with severe water scarcity, and around 1.2 billion individuals worldwide lack equitable access to clean drinking water [4]. As a consequence, ensuring the provision of clean and safe water poses a significant challenge and an immediate priority. To tackle the challenge of the low availability of clean water supply, the United Nations (UN) has launched the Sustainable Development Goals (SDGs) and created a framework for national action with water included in one of the goals (SDG 6: clean water and sanitation) to achieve a more sustainable and better future [5,6]. Sachs and coworkers further introduced six transformations as modular building-blocks to operationalize the SDGs emphasize water and waste management, revealing the importance of wastewater treatment in

* Corresponding author at: Faculty of Chemical Engineering & Technology, Universiti Malaysia Perlis (UniMAP), 02600 Arau, Perlis, Malaysia.
E-mail address: qhng@unimap.edu.my (Q.H. Ng).

https://doi.org/10.1016/j.jwpe.2025.106993
Received 24 November 2024; Received in revised form 8 January 2025; Accepted 11 January 2025
Available online 19 January 2025

achieving SDG 6 and realizing a sustainable future [7].

A significant proportion of the water pollutants emissions are industrial wastewater and contributed by anthropogenic activities [8]. Water pollutants or contaminants are generally classified as organic chemicals, toxic inorganic heavy metals, inorganic non-metallic matters, and microbial pollutants. The typical organic pollutants in water include organic dyes, pesticides, phenols, pharmaceuticals, personal care products, and endocrine disruptors [9]. Most of the organic pollutants are biologically toxic and can cause serious diseases such as cancer and genetic mutations [10]. Hence, removing the pollutants before discharging them into the environment is necessary. The inorganic toxic metallic elements consist of various heavy metals, for instance, lead, cadmium, chromium, copper, and mercury, which can be found in effluents exuded from a myriad of industrial activities running the gamut from mining, electroplating, tanning, to leather dyeing [2]. Exposure to heavy metal ions, even at low concentrations, can pose detrimental effects on human health, including the development of various types of cancers as well as neurological problems [11]. Inorganic non-metallic pollutants are compounds that contain no carbon or contain only carbon bound to elements other than hydrogen. Inorganic non-metallic pollutants consist of ammonia, sulfate, phosphate, and chlorides [12]. Excess ammonia (aquatic toxicity), sulfate (diarrhea diseases), phosphate (eutrophication), and chlorides (soil salinity) can result in adverse environmental and health impacts [12–14]. Moreover, the emerging of microbial pollution in water resources has drawn much attention from researchers due to the harmful effects or infections such as digestive, infectious, and skin diseases through drinking pathogenic contaminated water and involving in microbial-contaminated water recreational activities [15]. The primary and significant sources contributing to microbial pollution in water resources are land uses and human-driven activities associated with faecal pollution [16,17]. Thus, proper and efficient treatment for removing these pollutants is of immediate necessity. The conventional methods for removing contaminants from wastewater include precipitation, chemical oxidation, solvent extraction, membrane filtration, ion-exchange and adsorption [8]. It is worth highlighting that adsorption is one of the most efficient, economical, and facile methods compared to conventional techniques [18].

In recent years, there have been various conventional adsorbents, for instance, activated carbons, clay minerals, carbon nanotubes, zeolites and agricultural wastes, for removing hazardous pollutants from aqueous solution [19,20]. Most conventional adsorbents possess a large surface area, large porosity and well-defined surface functional groups, facilitating adsorption [21]. However, many of these adsorbents have suffered from low adsorption and desorption efficiency or lack of selectivity for target pollutants, limiting their practicality and commercialization [19,21]. Therefore, there is a growing tendency to utilize stimulus/stimuli-responsive smart materials that selectively adsorb target pollutants at a highly efficient rate.

Materials that respond to either internal or external stimulus/stimuli (pH, temperature, light and magnetic field) with dynamic change in their physicochemical properties are termed smart materials. They have witnessed and emerged for practical usage in the water treatment process due to their tuneable properties where the materials are designed to respond to desired stimulus/stimuli for enhancing the treatment process [22]. The selection of materials for constructing the smart adsorbents depends wholly on the intended end application, and whether the stimulus/stimuli inherent to the application system are suitable and enhanced the system. Smart responsive materials are more effective, easily tuneable, highly selective and exhibit various physicochemical characteristics such as thermal stability, high porosity, magnetic property and reusability [21]. In addition, the reversible attributes of smart materials promote effective regeneration by varying the respective stimulus/stimuli responses. Thus, they do not require toxic and costly organic solvents for regeneration purpose, reducing the possibility of secondary pollution. From a different perspective, smart materials exert self-cleaning properties that increase reusability and operation lifetime, which reduces overall operational costs.

This review highlights the recent advances in several categories of stimuli-responsive materials (thermal-, light-, magnetic- and pH-responsive) in the enhancement of the removal of organic chemicals, inorganic heavy metals, inorganic non-metallic matters and microbial pollutants. A particular focus is on developing novel dual- or multi-stimuli-responsive materials in environmental and water treatment applications. Moreover, the challenges and prospects concerning smart materials are also discussed. To the best of our knowledge, there is scarcely reviews have been done on using smart materials in environmental applications. Hence, this review aims to provide valuable insights and a comprehensive study on the possibility of using stimuli-responsive smart materials to remove organic, inorganic and microbial pollutants.

2. Single-stimulus responsive materials

2.1. Thermo-/temperature responsive smart materials

Thermo- or temperature-responsive smart materials possess a unique ability to change their physio-chemical properties reversibly in response to the thermodynamic environment [23]. They are mainly classified into two groups based on their temperature-responsive behaviour, namely upper critical solution temperature (UCST) and lower critical solution temperature (LCST), in which the materials demonstrate phase transition in specific small temperature intervals [24–26]. The UCST thermo-responsive materials can dissolve in solvents (hydrophilic) above the UCST and are insoluble (hydrophobic) below the UCST, and vice versa for LCST-type materials [27]. A well-known and studied thermo-responsive polymer, poly-N-isopropylacrylamide (PNIPAM) has its LCST at $\sim 32\ ^{\circ}C$, which it exhibits hydrophilic properties when the temperature is lower than its LCST and hydrophobic at a temperature above LCST [26,28]. The hydrophilic nature of PNIPAM at a temperature lower than its LCST is due to the exposed amide groups. Hence, it can form hydrogen bonding with water molecules and soluble in it. While at temperature above PNIPAM LCST, hydrogen bonds are broken due to more isopropyl groups are exposed, thus hydrophobic interaction is dominant [29]. This unique nature of PNIPAM provides an innovative idea for the adsorption/desorption of pollutants by varying system's temperature and self-cleaning ability towards the adsorbents in water treatment applications. Nowadays, PNIPAM-based thermo-responsive smart materials have attracted significant research attention due to their large volume phase transition, versatile functionalization potential, and LCST near ambient temperature [25,30,31]. The minimal energy required for phase transitions makes these materials highly suitable for cost effective and sustainable water treatment applications. Table S1 summarizes the findings of several PNIPAM-based thermo-responsive adsorbents for removing organic, inorganic and microbial pollutants.

The hydrophilic-hydrophobic phase transition nature of PNIPAM has been enlightening the expansion usage of PNIPAM and its composites for removing organic contaminants from water. Recently, Yang and the group [32] fabricated a P(NIPAM-*co*-AAc)/MoS_2 composite hydrogel using *N*-isopropylacrylamide (NIPAM) and acrylic acid (AAc) as monomers, and molybdenum disulfide (MoS_2) as functional particles for the removal of methylene blue (MB). The maximum adsorption capacity of the composite hydrogel can reach as high as 1258 mg/g at room temperature mainly owing to the cross-linked network structure carrying ionizable carboxyl groups —COO^- and negatively charged MoS_2 particles that can adsorb with the positively charged MB through electrostatic interaction. In addition, the organic dye MB molecules could also interact with PNIPAM hydrogel through hydrogen bonding, leading to an increment in the adsorption capacity. Besides, the thermo-responsive PNIPAM further exhibits its swelling state at room temperature, resulting in molecular chain stretchers that benefit the diffusion of MB dye molecules into the three-dimensional cross-linked network. However, the chain collapses above the phase transition temperature, and water is

expelled, causing the network structure to shrink and promote the desorption of dye molecules [32]. A similar application of PNIPAM to removal MB can be observed in the work of Pany and the team [33].

Moreover, PNIPAM and its composites also reported efficacy in the removal of methyl orange (MO) [34,35], rhodamine B (RhB) [28], malachite green (MG) [28] and Congo red (CR) [35]. It is noteworthy to emphasize the mixing of PNIPAM with graphene oxide (GO) by the work of Cao et al. [28] for the removal of organic dyes (rhodamine B (RhB), methylene blue (MB) and malachite green (MG)) reported excellent removal efficiency at temperature above the LCST of PNIPAM, which is contrary with the other organic dye removal studies. Such a phenomenon is attributed to the π-π stacking and hydrogen bonding interactions occurred between the dye molecules and GO when PNIPAM underwent conformational change at temperature above the phase transition temperature, leading the organic dye molecules previously bound only to PNIPAM to be pulled to contact with GO. Above the LCST of PNIPAM, water is expelled out from PNIPAM, while the organic dyes are encapsulated and enriched in the gel phase, leaving clean water behind in the aqueous phase [28]. Fig. 1 demonstrate the sol-gel transition of GO/PNIPAM mixed system for removing organic dyes at 25 °C and 40 °C.

The P(NIPAM-*co*-AAc)/MoS_2 composite hydrogel system has the advantage of being highly specific and effective for the removal of cationic dyes due to the presence of negatively charged MoS_2 particles, which is favourable for the water treatment that in needs this specificity. However, this specificity is also a disadvantage as it limits its interaction with other pollutants, reducing its versatility. In contrast, the GO/PNIPAM mixed system offers the benefit of greater flexibility by utilizing a phase transition mechanism above the LCST of PNIPAM. This extraction-like process harnesses hydrophobic interactions to efficiently adsorb and encapsulate the aromatic dyes, making it more versatile for the removal of other organic pollutants. Additionally, the P(NIPAM-*co*-AAc)/MoS_2 composite operates effectively at temperature below the phase transition point, while the GO/PNIPAM composite relies on PNIPAM conformational change at higher temperatures. Hence, the operational temperature and pollutant specificity are crucial considerations when selecting between these systems for different water treatment applications.

Apart from dyes, phenolic compounds are another persistent organic pollutant that endangers human health and the environment. Depending on the PNIPAM functionalized particles and adsorption mechanism, the optimal working temperature for removing phenolic compounds could be varied. For instance, Wang and coworkers [36] synthesized a 2-cyanoethyltriethoxysilane (CTES) bridged (6-tetraethylenepentamine-6-deoxy)-β-cyclodextrin (NH-β-CD) encapsulated MXene/PNIPAM to obtain MXene-CTES-β-CD/PNIPAM composite hydrogel that is effective for the adsorption of *p*-nitrophenol (4-NP) under room temperature. The adsorption capacity gradually decreased upon the increment of the solution temperature because the hydrogel's phase transition from hydrophilic to hydrophobic induces shrinkage in the overall volume, leading to less contact area with 4-NP and disrupting the hydrogen bonding in between [36]. In contrast, Tokuyama et al. [37] reported that the adsorption of bisphenol A (BPA) and 4-isopropylphenol performed better at temperatures above the LCST of PNIPAM using synthesized PNIPAM/silica gel composite. The phenolic compounds mentioned were adsorbed onto the gel composite via hydrophobic interactions and desorption of the organic compounds can be triggered by changing the media temperature across the LCST range to modulate the phase transition of PNIPAM. It is noteworthy to point out that when hydrophobic interactions are the primary mechanism for pollutant removal, less hydrophobic compounds exhibit lower adsorption capacities. For instance, the PNIPAM/silica gel composite demonstrated a lower amount of 4-isopropylphenol adsorbed compared to BPA under similar working conditions, as reported in the study [37].

For the removal of inorganic pollutants, a thermo-responsive poly(N-isopropyl acrylamide)-*block*-poly(acrylic acid) (PNIPAM-b-PAA) copolymer was synthesized through reversible addition-fragmentation chain transfer (RAFT) polymerization by the study of Kafetzi et al. [38] as a potential adsorbent for Cu^{2+} and SO_4^{2-}. The adsorption process of Cu^{2+} and SO_4^{2-} proposed was started with the binding of cationic Cu^{2+} ions to the carboxylate groups of PAA that carry anionic charges. Simultaneously, SO_4^{2-} ions interact with the positively charged amide groups of PNIPAM through electrostatic and hydrogen bonding interactions, followed by the hydrophilic-hydrophobic phase transition of PNIPAM induced via the increment of solution temperature above its LCST. The hydrophobic interactions between PNIPAM-b-PAA/Cu^{2+}/SO_4^{2-} assemblies at 60 °C form large aggregates that can be easily separated using filtration. In another study, Luo and coworkers synthesized an alginate-derived bead constituted of PNIPAM interpenetrated in alginate-Zr^{4+} network (PNIPAM/SA-Zr) decorated with polyethylene glycol (PEG) to remove or reduce the excessive amount of phosphorus discharging into water [39]. The role of PNIPAM in the bead is to enhance phosphorus adsorption capacity through its hydrophilic state at a temperature below its LCST, make the transportation of phosphate ions into the bead adsorption sites more easily at aqueous phase, and improve phosphorus desorption rate by de-swelling PNIPAM at a temperature above its LCST [39]. Furthermore, PNIPAM-*block*-4-vinylpyridine (PNIPAM-*b*-P4VP) showed remarkable heavy metals As (III) and Cr (VI) adsorption from aqueous solutions containing sodium arsenite ($AsNa_3O_3$) and potassium dichromate ($K_2Cr_2O_7$) [35].

Recently, Chen's group synthesized a novel antibacterial copolymer brush surfaces containing geminized cationic amphiphilic polymers ($pAGC_8$), and PNIPAM reported excellent bactericidal efficiency and self-cleaning ability [40]. The copolymer brush surface's capturing,

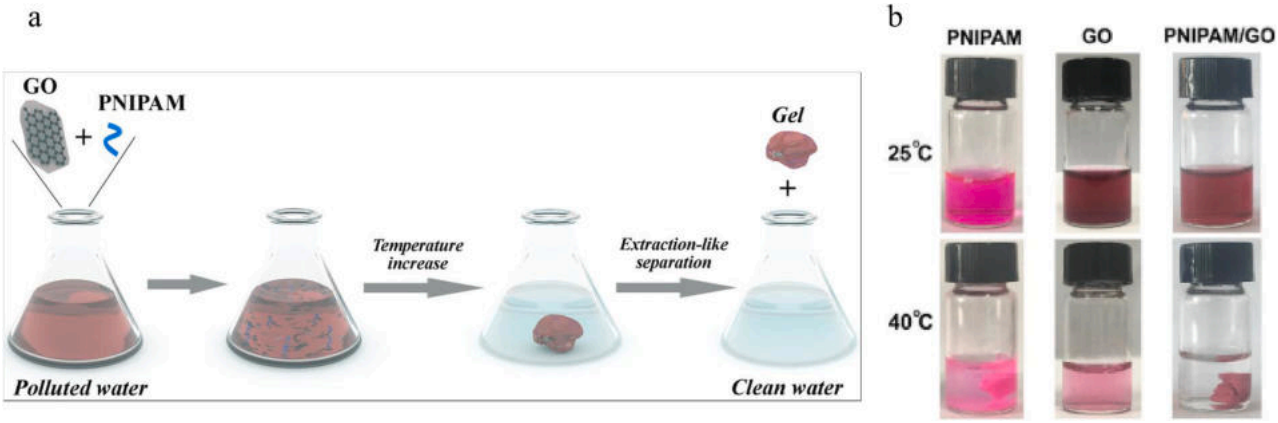

Fig. 1. (a) Sol-gel transition of GO/PNIPAM mixed system for removing organic dyes. (b) Photographs of PNIPAM, GO and PNIPAM/GO solution containing 50 mg/L of RhB at 25 °C and 40 °C [28]. Reproduced with permission from [28].

killing and releasing efficiency reached above 80 % for both *Staphylococcus aureus* (*S. aureus*) and *Escherichia coli* (*E. coli*). The antibacterial effect remained excellent after three consecutive cycles, benefiting from its excellent self-cleaning ability. Fig. S1 displays the action of self-cleaning ability of the copolymer brush surface via the phase transition of PNIPAM from varying the medium temperature. A similar application of PNIPAM in constructing an antibacterial copolymer brush can be referred to the work of Wang et al. [41]. In all discussed PNIPAM composite systems, pollutant adsorption and desorption are efficiently achieved by varying the temperature across the phase transition point. This approach eliminates the need for toxic chemicals or extensive washing processes typically required by conventional adsorbents, providing a more sustainable and environmental-friendly solution for water treatment.

2.2. Light responsive smart materials

Photocatalysts, the noble representative of Advanced Oxidation Processes (AOPs), are the best to express light responsive smart materials, with the light source needed to initiate the photocatalytic reaction [42]. Several semiconducting materials have been utilized as photocatalysts, and among all the semiconductors, titanium dioxide (TiO_2) is one of the most widely used and reported photocatalysts in the water treatment process. Such a scenario is owing to its superior photocatalytic activity, cost-effectiveness, availability, photostability, and non-toxicity nature [43–45]. The potent efficacy of AOPs in water pollutants removal comes from the in-situ production of strong and highly reactive hydroxyl radicals (•OH) and superoxide radicals ($O_2^{\bullet -}$), which can remove almost all inorganic and organic pollutants, including pathogenic microbes found in water resources and transform the pollutants into non-toxic products such as carbon dioxide (CO_2) and water (H_2O), initiated by a green source of light energy [46]. The production of the radicals mentioned above in TiO_2 is because of the electronic configuration of TiO_2 when irradiated with ultraviolet (UV) light where the electrons (e^-) from the valence band (VB) are excited to the conduction band (CB), forming energized holes (h^+). The holes (h^+) could react with water (H_2O) or hydroxyl ions (OH^-) to form the hydroxyl radicals (•OH), whereas the electrons (e^-) might react with oxygen (O_2) to form superoxide radicals ($O_2^{\bullet -}$) [47]. Both of the radicals participate in the redox reaction of transforming the contaminants into non-toxic products such as carbon dioxide (CO_2), water (H_2O) and inorganic mineral ions [46]. A simple mechanism of semiconductor photocatalysis is shown in Fig. S2.

Unfortunately, some limitations restrain the application of TiO_2 in water treatment, including (1) the wide band gap energy of ~ 3.2 eV leads to a narrow range of UV light absorption, (2) the high recombinant rate of the excited electrons (e^-) and holes (h^+), and also (3) low electrical conductivity and pore BET surface area results in slow photocatalytic reaction rates [48–51]. Hence, the challenges and primary goal of TiO_2 development are addressing the mentioned limitations to convert the fundamental basic research into a successful innovation with the possibility of implementing the green innovative materials into real-life water treatment.

Moving forward to the direction of green chemistry, Ngoepe and coworkers synthesized TiO_2 nanoparticles using the green route of *Monsonia burkeana* (*MB*) plant extract for the removal of methylene blue (MB) [52]. Although an excellent 85.5 % of MB was photocatalytic degraded, the synthesized TiO_2 nanoparticles still face the wide band gap (3.53 eV) concern, which the catalytic process only initiated with UV light irradiation. UV light only constituents a small portion (~5 %) of sunlight, thus, it is a waste and less energy efficient in exploiting the inexhaustible clean source of light energy [48]. Tons of effort have been made to overcome the limitations of TiO_2. Among the approaches, metal or non-metal doping and forming composites with suitable supportive materials are considered effective ways to enhance the photocatalytic activity of TiO_2. Doping with elements, such as carbon [53], silver [54], nitrogen [55], oxygen [55] and fluorine [56] aids in producing ionic defects and impurity energy levels in TiO_2 crystal lattice, which the ionic defects can act as a reservoir for the photogenerated carriers diminishes the recombination of photogenerated electron-hole pairs. Meanwhile, the impurity energy levels would provide donor or acceptor sites in the band gap, leading to the extension of visible light absorption over TiO_2 [56].

Although both metal and non-metal doping enhance the photocatalytic performance of TiO_2 through band gap tuning and reduced charge recombination. Non-metal doping, such as nitrogen doping, also improves the surface properties of TiO_2, enhancing pollutant adsorption. For instance, the carbonized TiO_2-coated melamine foam (CTiMF) studied by Lu and the team [55] contains nitrogen-doped carbon with hydrophilic properties, enabling it to effectively soak up dye solutions and improve adsorption. In contrast, a key drawback of metal doping, such as silver doping [54], is the potential leaching of toxic metal ions into the environment, which raises concerns for sustainable environmental applications. Coupling TiO_2 with suitable supportive materials could significantly increase its active sites surface area while providing attractive mechanical strength and thermal stability [57,58]. For instance, Lu and the team have successfully immobilized TiO_2 nanoparticles on melamine foam via a biomimetic polydopamine (PDA) coating followed by a carbonization treatment as a promising sunlight-driven degradation strategy for removing rhodamine B (RhB) and traditional dyeing wastewater [55].

Under the doping approach, Gao and his coworkers [53] have reported an idea of coating a very thin (1 nm) layer of carbon onto the surface of TiO_2 (TiO_2@C) in which the results revealed that it shows non-selective adsorption in both UV and visible light, enhancing the separation of the photogenerated carriers and impressive performance in degrading methylene blue (MB) and tetracycline (TC). The incorporation of the carbon layer onto the surface of TiO_2 contributed to an extension of the adsorption region from UV to visible light. Furthermore, the excellent hydrophobicity of carbon makes TiO_2@C particles to stay afloat on the surface of liquid in which TiO_2 could receive the maximum sunlight, which is beneficial for photocatalysis performance (Fig. 2a). By referring to electrochemical impedance spectroscopy (EIS) of both TiO_2 and TiO_2@C, carbon coated TiO_2 (TiO_2@C) demonstrates a lower electron transfer resistance than TiO_2, which indicates that the carbon layer provides a route for transferring the excited electrons and improves the separation of photogenerated carriers. The synergy effects of TiO_2@C greatly enhanced the photocatalytic activity in degrading MB when compared with pure TiO_2 under dynamic conditions that resemble the actual situation of a water treatment plant (Fig. 2b and c).

It is noteworthy to mention the multiple-element co-doping strategy of nitrogen and fluorine applied on TiO_2 ((N, F)-co-doped $TiO_{2-\delta}$ nanofibers (FTO)) as demonstrated by the work of Chen et al. [56] for the removal of Cr (VI). The synergistic effects of co-doping could be visualized directly in the broadening of the absorption light region to visible light and improvement in the transfer ability of the photogenerated carriers, yielding even more significant enhancement in the photocatalytic performance of TiO_2 materials compared to those achieved with the single-element doping approach. The as-prepared FTO sample performs well in the photo-reduction of Cr (VI), where 31 % of Cr (VI) was removed under visible light irradiation within 60 min, while the commercial TiO_2 only achieved 11 % of Cr (VI) removal efficiency. For the removal of microbial pollutants, Moradi and co-workers [59] evidenced the efficient photocatalytic inactivation performance of TiO_2 anchored in natural pyrite (TiO_2NP) in the elimination of *Escherichia coli* (*E. coli*). The photo-efficiency and response of TiO_2 were enhanced using the narrow band gap semiconductor, natural pyrite (NP), and acts as an effective light harvester to improve from UV to visible light absorption. In addition, the photogenerated electrons of NP can be transferred to the conduction band of TiO_2, providing an efficient electron-hole pairs separation route in the TiO_2NP nanoparticles, further contributing to the amelioration of photocatalytic inactivation performance. This study also

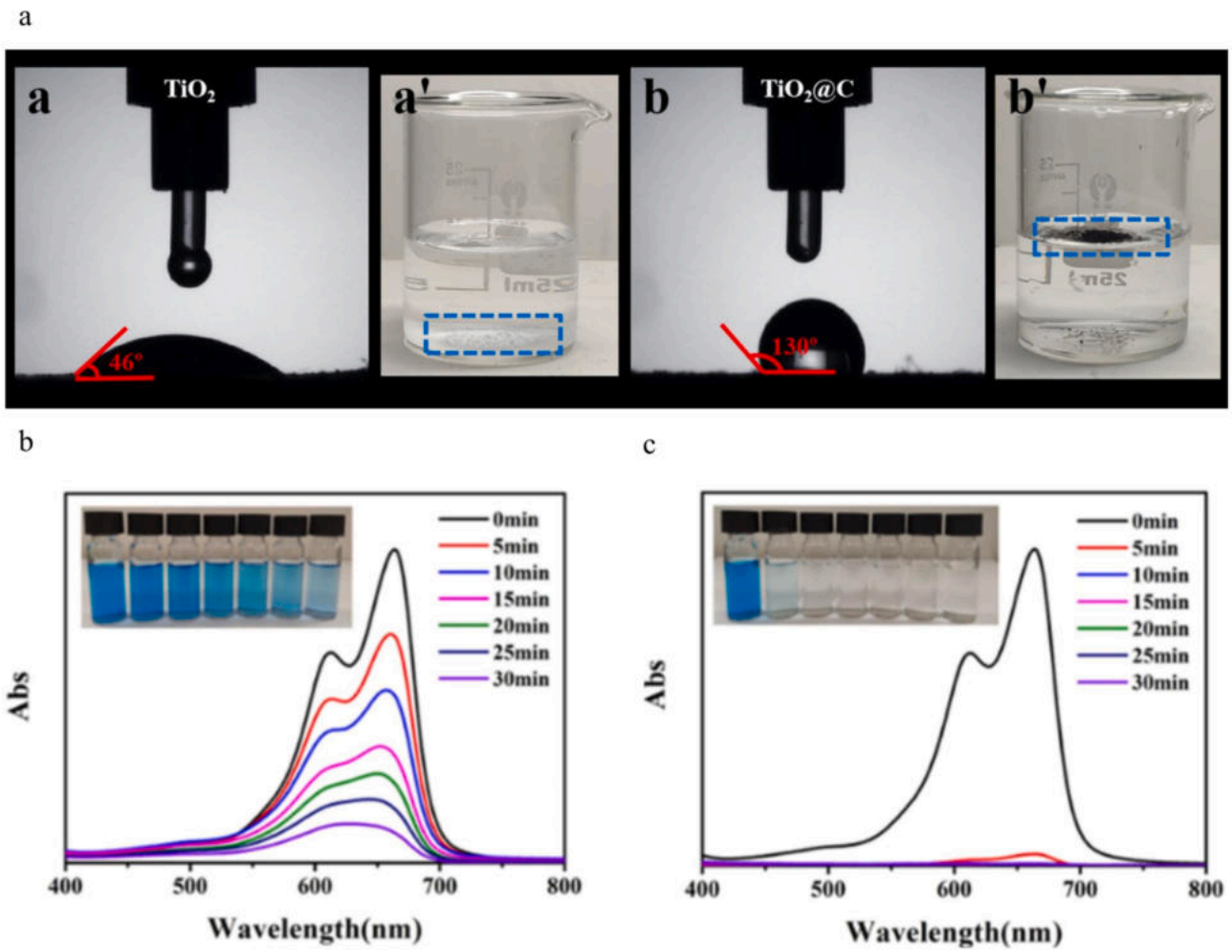

Fig. 2. (a) Schematic diagram of the water contact angle (a, b) and hydrophobicity (a′, b′), and photocatalytic activity in degrading methylene blue (MB) under dynamic condition of (b) TiO_2 and (c) TiO_2@C [53]. Reproduced with permission from [53].

revealed that several parameters including pH, catalyst dosage, TiO_2NP ratio, bacterial concentration, aeration, inorganic ions and natural organic matter significantly affect *E. coli* removal rate. Table S2 briefly overviews the reported TiO_2-based light-responsive smart materials for water treatment applications.

Besides all the complex works applied to TiO_2, researchers are also trying to search for alternatives with excellent photocatalytic properties. Among the options, polyoxometalates (POMs), the clusters of anionic metal oxide comprised of oxygen atoms, linked together by early transition metals (usually molybdenum (Mo), tungsten (W), vanadium (V), niobium (Nb) or tantalum (Ta)) at their highest oxidation state regarding the addenda atoms and traces amount of heteroatoms (usually Si, P, S or Ge), have received much attention as photocatalysts [60,61]. Their high electronegativities (enriched with oxygen surface atoms), controllable morphology, reversible multiple electron redox properties, high thermal stability, and tuneable band gap structures made them favourable alternatives [62,63]. In addition, POMs exhibit similar semiconductor features with light absorption and regulated energy levels (VB and CB of semiconductor) [64]. There are a few commonly designed structures of POMs, namely Keggin, Dawson, Lindqvist, Preyssler, and Anderson as shown in Fig. S3, based on their difference in the coordination number [65]. However, the in-depth explanations regarding the morphology and physicochemical properties are beyond the scope of this review.

Most recently, Lai et al. [66] summarized the limitations of POMs that hampered their superiority after reviewing the applications of POMs in the remediation of organic wastes, whereby the limitations including large band gap energy, least active sites (small surface area), structural stability in alkali-prone solution and recoverability issue. Anchoring POMs into metal-organic frameworks (MOFs) has attracted much interests in tackling the shortcomings of POMs, as mentioned above. MOFs are organic-inorganic hybrid materials synthesized through the linkage of metal ions with organic ligands arranged orderly in topological structure with ultrahigh porosity [66,67]. Due to these fascinating structures and physical properties of MOFs, they are beneficial in enhancing the stability of POMs in harsh conditions, while providing a large surface area for the active sites of pollutant adsorption. Moreover, POMs could be recycled easily as heterogeneous catalysts by incorporating MOFs as support materials. For example, Zhao et al. [68] synthesized and fully characterized two stable 3D polyoxometalate-based metal-organic frameworks (PMOFs in short) with different POMs precursors, namely $[Cu^{I}_{12}(trz)_8(H_2O)_2][\alpha\text{-}SiW_{12}O_{40}] \cdot 2H_2O$ (1) and $[Cu^{I}_{12}(trz)_8Cl][\alpha\text{-}PW_{12}O_{40}]$ (2). As a result of the difference in anionic charge and bonding capabilities of the two POMs precursors ($[\alpha - SiW_{12}O_{40}]^{4-}$ and $[\alpha - PW_{12}O_{40}]^{3-}$), thus it showed unique framework structures even under similar preparation conditions where the polyoxoanions (POAs) in 1 are located in the nine-membered rings of Cu-trz, while POAs in 2 are lying in the adjacent layers through the weak interactions between Cu and O (Fig. 3a). The inclusion of Cu metal into the amalgamation is to widen the adsorption spectrum to the visible light region, and this was supported with low band gap energy where 2.11 eV and 2.35eV were reported for PMOF 1 and 2, respectively. In

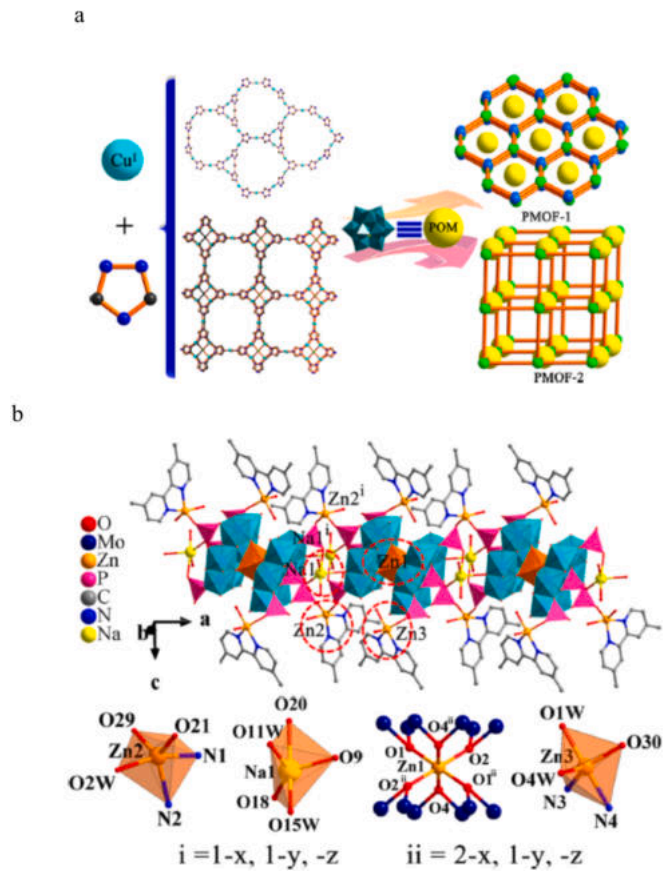

Fig. 3. (a) Schematic diagram of the formation processes for PMOFs 1 and 2 [68]. (b) Polyhedral and ball-stick representations showing the 1D chainlike structure in hourglass-type based molybdphosphate hybrid 2 [69]. Adapted with permission from [68] and [69]. Copyright 2018 and 2019 American Chemical Society.

addition, the metal-organic ligand unit, {Cu^{I}(trz)} acts as a POM linker and enhances the photocatalytic activity by transferring the excited electrons from one POM to another. The unique framework structures and difference in band gap energy significantly affect the photodegradation efficiency of Rhb dye in which the conversion rate recorded for PMOF 1 and 2 were 91 % and 81 %, respectively, under irradiation of visible light for 240min. Such observation was attributed to the skeleton of PMOF 2 that is not beneficial in transporting the promoted electrons to the surface, hence retards the generation of hydroxyl and superoxide radicals. Lower band gap energy indicates PMOF 1 is more accessible to photo-activate than PMOF 2. Moreover, PMOF 1 showed no apparent loss in activity after five cycles of photodegradation, demonstrating its good reusability and stability.

In addition to MOFs, coupling POMs with semiconductors (TiO_2) also noted with enhancement in photocatalytic performance as the combination of both POMs and TiO_2 not only prevent the recombination of excited electrons (e^-) and holes (h^+) that happened in TiO_2, but also facilitates the generation of photogenerated carriers with POMs semiconductor-like features and multiple electron redox properties [70–72]. However, due to both POMs and TiO_2 having wide band gaps that limit its application under UV light irradiation. With an effort to extend the adsorption region and further improve the photocatalytic activity, lots of attempts have been made to synthesize plasmonic photocatalysts by incorporating noble metals such as Ag [73], Au [74], and Pt [75] into POMs/TiO_2-based photocatalysts.

For instance, Shi et al. [73] had synthesized a novel POM-TiO_2 composite loaded with Ag nanoparticles showed noticeable enhancement in photodegradation and photoreduction of methyl orange (MO) and Cr (VI), respectively. The highest photocatalytic performance achieved by PMo_{12}/TiO_2/Ag composite catalysts were reported with an Ag weight percentage of 5.41 % (denoted as PMo_{12}/TiO_2/Ag-5.41), MO can be degraded entirely in 120 min under visible light irradiation. The increment of Ag content in the composites from 0 % to 5.41 % resulted in promoting the photocatalytic activity; however, further loading of Ag nanoparticles started to bring negative effect as the excessive Ag nanoparticles occupied the active sites on the surface of PMo_{12}/TiO_2 nanofibers, thus reducing the adsorption capability and the formation of active photogenerated species. The influence of noble metal Ag nanoparticles on the photocatalytic performance is related to the surface plasmonic resonance (SPR) and the intense local electromagnetic fields of Ag nanoparticles, which promote the visible light response and reduce the photogenerated charge recombination, resulting in the enhancement of the photocatalytic activity of the composite [73]. Consistently, the introduction of Ag nanoparticles reported enhancement in the photoreduction of Cr (VI), with about 79.10 % have been reduced by PMo_{12}/TiO_2/Ag-5.41 in 60 min under visible light irradiation. For the reusability of PMo_{12}/TiO_2/Ag-5.41, it recorded no noticeable loss of the photocatalytic performance after four reuse cycles.

In comparing noble metal incorporation methods, Guan et al. [75] fabricated a Pt-$TiO_2/H_3PW_{12}O_{40}$ film with Pt nanoparticles enclosed within a TiO_2 and $H_3PW_{12}O_{40}$ as a measure to minimize the leaching of toxic noble metals into the environment. This contrasts with the PMo_{12}/TiO_2/Ag composite, where Ag nanoparticles were photodeposited on the surface PMo_{12}/TiO_2 nanofibers, increasing the risk of potential leaching. While enclosing Pt is unavoidable to lose certain degree of the SPR effect because the covered noble metal limits light absorption efficiency. Yet, the Pt-$TiO_2/H_3PW_{12}O_{40}$ catalyst still achieved 100 % degradation of 2-chlorophenol (2-CP), 2,4-dichlorophenol (2,4-DCP), and 2,4,6-trichlorophenol (2,4,6-TCP) in single systems within 240 min under simulated sunlight irradiation. Additionally, it retained 95.5 % degradation efficiency after three consecutive cycles with minimal leaching of Pt (0.02 %) and $H_3PW_{12}O_{40}$ (0.11 %), demonstrating superior stability and environmental safety compared to the PMo_{12}/TiO_2/Ag composite, where Ag nanoparticles leaching remains insufficiently studied.

In a different approach, Hou and the team [69] have been hydrothermally synthesized three highly reduced hourglass-type {Zn$[P_4Mo_6O_{31}]_2$}$^{22-}$ based molybdophosphate hybrids with the formulas of $[Zn(mbpy)(H_2O)_2]_2[Zn(mbpy)(H_2O)]_2${$Zn[P_4Mo_6O_{31}H_7]_2$}$\cdot 9H_2O$ (1), $[Na(H_2O)_2]_2[Zn(mbpy)(H_2O)_2]_2[Zn(mbpy)(H_2O)]_2${Zn$[P_4Mo_6O_{31}H_6]_2$}$\cdot 15H_2O$ (2) and (H_2mbpy){$[Zn(mbpy)(H_2O)]_2[Zn(H_2O)]_2$}{$Zn[P_4Mo_6O_{31}H_6]_2$}$\cdot 10H_2O$ (3) as photocatalysts for the photoreduction of Cr (VI). Such reduced-state and hourglass-type POMs are constructed by connecting two identical half units of $[P_4Mo_6O_{31}]^{12-}$ (abbreviated as {P_4Mo_6}) with a bridged metal M in a centrally antisymmetric manner. Hourglass-type cluster POMs have enriched electrons and a broader absorption spectrum that extends into the visible or near-infrared range, significantly enhancing their photo-adsorption capacity and sunlight utilization [76]. On the basis of hourglass-type POMs, ZnO and 4.4′-dimethyl-2,2′bipyridine (mbpy) were further incorporated to improve the hybrid complexes visible light sensitivity and maintain structure stability. Among the three complexes, hybrid 2 displayed the highest removal ratios of Cr (VI), owing to its structure (as shown in Fig. 3b), effectively suppressing the recombination of photogenerated carriers, resulting in a notably higher photocatalytic efficiency. Such a result again demonstrates the importance of building block packing arrangement in the complexes of photocatalysts and that much consideration needs to be taken during fabrication to maximize and achieve superior photocatalytic performance.

Another similar application of hourglass-type POMs-based crystalline materials as efficient cooperating photocatalysts was reported by Tian and coworkers [76] for the reduction of Cr (VI) and removal of organic methylene blue (MB) dye. The work consistently illustrated that the structural and composition differences can affect the photo-

absorption capacity and photogenerated electron-hole pairs recombination probability, thereby influencing the optical and photocatalytic performance of the catalysts. It is noteworthy to point out that the mixed pollution system that consists of both Cr (VI) and MB provides a synergistic effect in improving the photocatalytic efficiency as the photogenerated electrons and holes by the photocatalysts under visible light excitation can respectively undergo Cr (VI) reduction and MB degradation, which incidentally achieving the separation of charges.

To access the photocatalytic bacterial inactivation performance of POMs, Lafta et al. [77] prepared a photocatalyst composite (g-C_3N_4/PTA) by immobilizing high redox ability of phosphotungstic acid (PTA, a stable Keggin structure of POMs) on metal-free graphitic carbon nitride (g-C_3N_4) for the removal of *Escherichia coli* (*E. coli*). The findings showcased that *E. coli* photodegradation was enhanced, with the g-C_3N_4/PTA exhibited the best photocatalytic performance of 92 % under visible light irradiation for 180 min when compared to unmodified g-C_3N_4 and PTA. The enhancement in photocatalytic efficacy was attributed to the synergistic of g-C_3N_4 and PTA in the synthesized hybrid, in which the photogenerated electrons from the conduction band of g-C_3N_4 can be trapped by the PTA molecules promoting the separation of photogenerated electrons and holes, and thus, improving the photocatalytic performance.

Most recently, Ammar and colleagues [78] demonstrated the idea of piezophotocatalytic degradation towards *Staphylococcus aureus* (*S. aureus*) using the synthesized heterogeneous composite of phosphomolybdic acid (PMA) acid immobilized onto g-C_3N_4 (g-C_3N_4/PMA) as the photocatalyst. It is worth highlighting that the addition of mechanical stress induced via ultrasonic vibration simultaneously with visible light illumination remarkably enhanced the bacterial inactivation, with piezophotocatalytic inactivation efficiency being the highest at 94.2 % followed by 91 % of photocatalytic and 87.7 % of piezocatalytic inactivation activities. The piezopotential induced by the mechanical stress advocates the formation of electric field in the piezoelectric materials, modifying the energy state across the piezomaterial and promoting the efficient separation of photo-produced carriers, consequently enhancing the photocatalytic performance [78,79]. Table S3 surmises the findings of reported POMs-based light-responsive smart materials for water treatment applications.

Conclusively, the best representative of photocatalysts which are both TiO_2 and POMs with superior photocatalytic performance and pollutant removal efficacy meet the idea of green material or technology that can be utilized in water purification and treatment. However, large band gap energy, recombinant on e^-/h^+ pairs and least active sites are among the most common limitations that exist in every semiconductor, including TiO_2 and POMs. Hence, lots of different attempts have been made and reported with the purpose of solving those limitations and, at the same time, enhancing the contaminant removal performance. One major drawback of photocatalysts is the significant reduction in photocatalytic performance in the presence of certain inorganic salt ions, such as sulfate and nitrate ions [55,80]. These ions act as scavengers of electrons and reactive radicals, effectively quenching the radicals generated during the photocatalytic process and thereby inhibiting pollutant degradation. Hence, strategies such as surface modification or forming photocatalyst composites with enhanced resistance to ion interference could be explored. Further, constructing a multifunctional composite that could work on multiple types of pollutants in only single-step water purification is a current emerging trend in the water treatment field, in which it is facile, fast and practical in real-life application. More and more future works should focus on synthesizing high pollutant removal efficacy and multiple functionalities photocatalysts with upscaling and long-time usage possibilities to meet the minimal industrial requirements. Thus, photocatalysts' recoverability is another vital factor, which will be discussed in the following section.

2.3. Magnetic responsive smart materials

In the downstream of the water treatment process, separation or recovery of adsorbents, catalysts, or composites from clean water effluent is considered an equally crucial part of preventing secondary pollution during disposal, which has adverse effects on aquatic life and human health [81,82]. For instance, additional solid-liquid separation steps, such as centrifugation and filtration, are required to separate the sorbents in the post-water treatment process [83]. Such an extra need brings complexity, energy consumption, and costs to the process design. In this regard, magnetic responsive materials provide a more sophisticated and promising way to resolve the above-mentioned recovery issue.

Magnetic nanoparticles (MNPs) are favourable for this environmental application mainly owing to their high surface area-to-volume ratio, low cost, rapid kinetics and superparamagnetic behaviour, resulting in facile and rapid separation by applying an external magnetic field [84]. In general, MNPs act as either direct purification agents (naked MNPs) or magnetic carriers (functionalized MNPs) for another active phase [85]. Although a high surface area-to-volume ratio is an attractive physical property for an adsorbent, the small particle size of naked MNPs possesses high surface energies. Hence, the MNPs aggregate into bulky particles form to minimize the surface energies and achieve a more stable state [86]. Moreover, the interactions between the particles, namely Van der Waals and magnetic dipolar forces, further promote aggregation or colloidal instability [87]. These factors subsequently negatively impact adsorption efficiency, such as reducing exposed specific active sites. Considering the mentioned drawbacks and numerous reviews that have been done on naked MNPs as active agents for various pollutant removal [84,85,88], this section will emphasize the functionalized MNPs with enhanced removal efficiency on organic, inorganic and as well as microbial pollutants.

The current research focuses on using MNPs as a novel adsorbent for dye removal. For instance, MNPs doped or coated with poly(sodium 4-styrene sulfonate) (PSS) [89], multi-walled carbon nanotubes (MWCNTs) [90] and clay in cross-linked of chitosan beads [91] have reported improvement in methylene blue (MB) uptake efficiency. The enhancement of MB removal efficiency resulted from the highly negative surface charge of PSS, MWCNTs and clay over a wide pH range. Hence, they promote an efficient electrostatic interaction between the functionalized MNPs and the cationic MB dye. Besides, PSS, MWCNTs and clays aid in sustaining the colloidal stability of MNPs, where the electrostatic repulsion takes place in the coated adlayers that restricts the agglomeration among MNPs, as shown in Fig. S4a with PSS as the example. Hence, MNPs functionalized with PSS, MWCNTs and clays have larger adsorption active sites when compared with naked MNPs, which is another contributing factor to the improvement of MB removal efficiency (Fig. S4b with PSS-coated MNPs as the example). Entrapping MNPs and clays in cross-linked chitosan beads is an extra benefit, as the magnetic beads can also adsorb anionic methyl orange (MO) dye (refer to Fig. S4c). Such observation is owing to the protonated cationic form of MNPs and amino groups of chitosan in the pH range of 3–5, which is advantageous in real-life applications as the wastewaters contain multiple pollutants with different behaviours. All the functionalized MNPs demonstrated sufficient magnetic recovery under an external magnetic field. However, the pH of the medium plays a critical role in influencing the magnetic recovery response. For instance, Lee and his co-workers [90] reported that MNPs functionalized with MWCNTs (n-MMWCNTs) exhibited immediate magnetic responsiveness at pH 3 and 7. In contrast, n-MMWCNTs displayed a slower response to the magnetic field at pH 9. Such an observation is attributed to the formation of a more stable and well-dispersed colloid at pH 9, as supported by the highest negative zeta potential of n-MMWCNTs at this pH. The increased negative zeta potential generated strong repulsive forces among the composite particles with $—OH^-$ and $—NO_3^-$ ions, resulting in delayed magnetic recovery.

Like cationic dye adsorption, the removal of anionic dye is also dominated by surface charge electrostatic interaction. Yang and his co-

workers [92] have reported an efficient and high selectivity for the adsorption of anionic alizarin red (AR) and acid orange II (AO) dyes that mixed with cationic malachite green (MG) and thionin acetate (TA) respectively by using a poly(ionic liquids) (PILs) functionalized magnetic nanosorbents. The adsorbent was prepared by grafting PILs onto silicon-coated Fe_3O_4 via Cu(0)-mediated reversible-deactivation radical polymerization (RDRP), as presented in Fig. S5a. The bulk cationic units in PIL through the entire pH range from 3 to 12 were the active species that effectively bonded with the anionic dyes while rejecting the cationic dyes due to electrostatic repulsion (Fig. S5b and S5c). The pH-stable cationic property of PIL is beneficial as pH fluctuation of water sources is a common issue confronted in water treatment. There was a noticeable reduction in magnetic saturation from naked Fe_3O_4 was measured at 64.5 emu/g, which decreased to 55.3 emu/g for Fe_3O_4@-SiO_2 and further to 37.2 emu/g for Fe_3O_4@SiO_2@PIL. This reduction in saturation magnetization values is due to the non-magnetic coatings and grafting of silica and PIL. Despite the decrease, the final adsorbent retained sufficient magnetic responsiveness to enable efficient magnetic separation.

Moreover, MNPs functionalized with catechol and branched polyethylenimine (PEI) (Fe_3O_4@catechol/PEI) [93], and 3-glycidoxypropyltrimethoxysilane (GPTMS) and poly-lysine (P-Lys) (Fe_3O_4@GPTMS@P-Lys) [94] also possess selectivity in the adsorption of anionic dyes. This specificity of both adsorbents is due to the protonated amino groups under acidic condition that give them positive charges and facilitate adsorption with anionic dyes. Similarly, a reduction in saturation magnetization values was observed upon the functionalization with non-magnetic counterparts. Yet, all the final adsorbents maintained strong magnetization, enabling rapid response and efficient collection under an external magnetic field. This magnetic-responsive property allowed the composites to be easily collected and reused over several consecutive cycles, retaining high removal efficiency with minimal adsorbent loss.

Unlike common adsorbents, functionalized MNPs have greatly enhanced the removal or separation of highly toxic and non-degradable heavy metals from water sources that negatively affect public health and the environment. Among the heavy metals, lead (Pb^{2+}) and cadmium (Cd^{2+}) are widely utilized in various industries such as metal plating, smelting, mining, cadmium-nickel and lead batteries, textiles and paint industries [95]. For instance, both Pb^{2+} and Cd^{2+} were effectively eliminated from water by MNPs modified with amino and carboxymethylated lignin (Fig. 4a) [96], sulfonated groups (Fig. 4b) [97] and encapsulation of MNPs into poly(vinyl alcohol) (PVA) and sodium alginate (SA) forming bio-magnetic membrane capsules (BMMCs) (Fig. 4c) [98]. The improvement in the heavy metals uptake capacity and efficiency was mainly due to the advantage of MNPs surface functionalization that provides abundant active sites, which have high affinity with Pb^{2+} and Cd^{2+} such as carboxyl (—COOH), hydroxyl (—OH), thiol (—SH) and sulfonic (—SO_3H) groups. The adsorption mechanisms of removing the mentioned heavy metals are all mainly attributed to ion exchange, hydrogen bonding and electrostatic interaction. All findings were well connected with adsorption performance at near-neutral pH conditions and reported the best overall adsorption efficiency and capacity. This is probably due to the protonation of carboxyl, hydroxyl, thiol and sulfonic groups at acidic conditions, forming competitive adsorption between the proton (H^+) ions and the heavy metal ions in the solution. Conversely, at alkaline conditions, the decrement in heavy metal ions removal might be due to the possible formation of metal precipitation for both Pb^{2+} and Cd^{2+} ions. Thus, this brings extra merit to the practicality of the functionalized MNPs as only mild conditions are required, and at the same time, providing magnificent adsorption performance on highly toxic heavy metals. Notably, the magnetic properties of sulfonated modified MNPs (Fe_3O_4-SO_3H MNPs) and BMMCs remained stable over multiple adsorption-desorption cycles, ensuring consistent recovery and reusability under an external magnetic field even after prolonged use.

Besides removing heavy metals, Xu et al. [99] reported the simultaneous removal of common non-metal inorganic pollutants, ammonia (NH_4^+) and phosphate (PO_4^{3-}), using green synthesized iron oxide nanoparticles dispersed onto zeolite to form EL-MNP@zeolite. At an initial concentration of 10mg/L each for the two co-existing ions, the material achieved removal efficiencies of 43.3 % for NH_4^+ and 99.8 % for PO_4^{3-}. Ammonia removal was mainly via physical adsorption, driven by electrostatic attraction between the negatively charged zeolite and positively charged NH_4^+ ions. In contrast, phosphate removal was primarily via chemisorption, involving ligand exchange between surface hydroxyl groups (Fe-OH) on EL-MNP@zeolite and phosphate ions, forming $FePO_4^{2-}$ complexes. While the iron oxide nanoparticles were incorporated to provide magnetic separation for recovery.

The emergence of microbial pollution and antibiotic-resistance microorganisms has attracted interest in developing an alternative and effective antimicrobial method for water treatment. Silvia et al. [100] and Seerangaraj et al. [101] have demonstrated biosynthesis of iron oxide nanoparticles (IONPs) from leaf extracts of *Cynometra ramiflora* and *Ruellia tuberosa*, respectively, that show excellent antimicrobial activity on both Gram-negative (*Escherichia coli* (*E. coli*), *Klebsiella pneumonia* (*K. pneumonia*)) and Gram-positive (*Staphylococcus aureus* (*S. aureus*), *Staphylococcus epidermidis* (*S. epidermidis*)) bacteria. The bactericidal effect of IONPs is due to the extra small size of the particles that can penetrate into the cells and cause damage to the cell membrane, leading to lysis of the bacterial cells. Besides, synthesizing IONPs from leaf extracts is beneficial because of the synergistic antibacterial activity of its phytochemical components that act as bacterial DNA inhibitors.

To further enhance the microbial removal efficiency of MNPs, mechanisms of both capture and inactive microbes play a vital role. For instance, MNPs functionalized with an antibacterial agent, cetyltrimethylammonium bromide (CTAB) (Fe_3O_4@CTAB) showed ultrafast capture and effective antibacterial effect on both Gram-negative *Escherichia coli* (*E. coli*) and Gram-positive *Bacillus subtilis* (*B. subtilis*) bacteria [102]. The ultrafast cell capture attribute of Fe_3O_4@CTAB is owing to the positive charged CTA^+ could interact with the bacteria that carry negative charges when the solution pH exceeds 4. Moreover, hydrogen bonding interactions between the carboxyl oxygen of the bacterial cell membrane and the quaternary ammonium of CTAB, and hydrophobic interactions between the methyl side chains of the cell membrane and the carbon chains of CTAB might also contribute to the efficient cell capture behaviour of Fe_3O_4@CTAB. After quick capture of bacterial cells, CTAB would then interfere with the internal respiratory enzymes of bacterial via the generation of reactive oxygen species (ROS) such as superoxide and hydrogen peroxide that damage the protein and DNA of the bacteria, eventually leading to cell death. In addition, Raghu and the team [103] utilized the large surface area advantage of graphene oxide (GO) and combined it with Fe_3O_4 reported better antibacterial activity against Gram-negative (*Pseudomonas aerugino* (*P. aerugino*), *Salmonella typhimuriumupon* (*S. typhimuriumupon*)) and Gram-positive (*Staphylococcus aureus* (*S. aureus*), *Bacillus subtilis* (*B. subtilis*)) when compared with bare Fe_3O_4. In another approach, tryptophan was used as a coating material to modify the surface properties of MNPs with N-[3-(Trimethoxysilyl)propyl]-ethylenediamine (TSPED) as cross-linking agent exhibits great antibacterial property against *E. coli* and *B. subtilis* [104]. This is due to the hydrogen bonding interaction between OH groups carried by tryptophan and the water molecules forming stable colloidal dispersion that facilitates the interaction with the bacterial cells. Furthermore, substantial interaction also promotes the production of ROS that beneficial in inducing oxidative stress on the cells. All these studies well demonstrate that MNPs or IONPs can serve as either active antimicrobial agents, utilizing their extremely small size to penetrate bacterial cells and induce lysis, or act as magnetic carriers for other antimicrobial agents, providing rapid magnetic separation for efficient recovery and reuse of the adsorbents.

Conclusively, magnetic responsive is a powerful, cost effective and

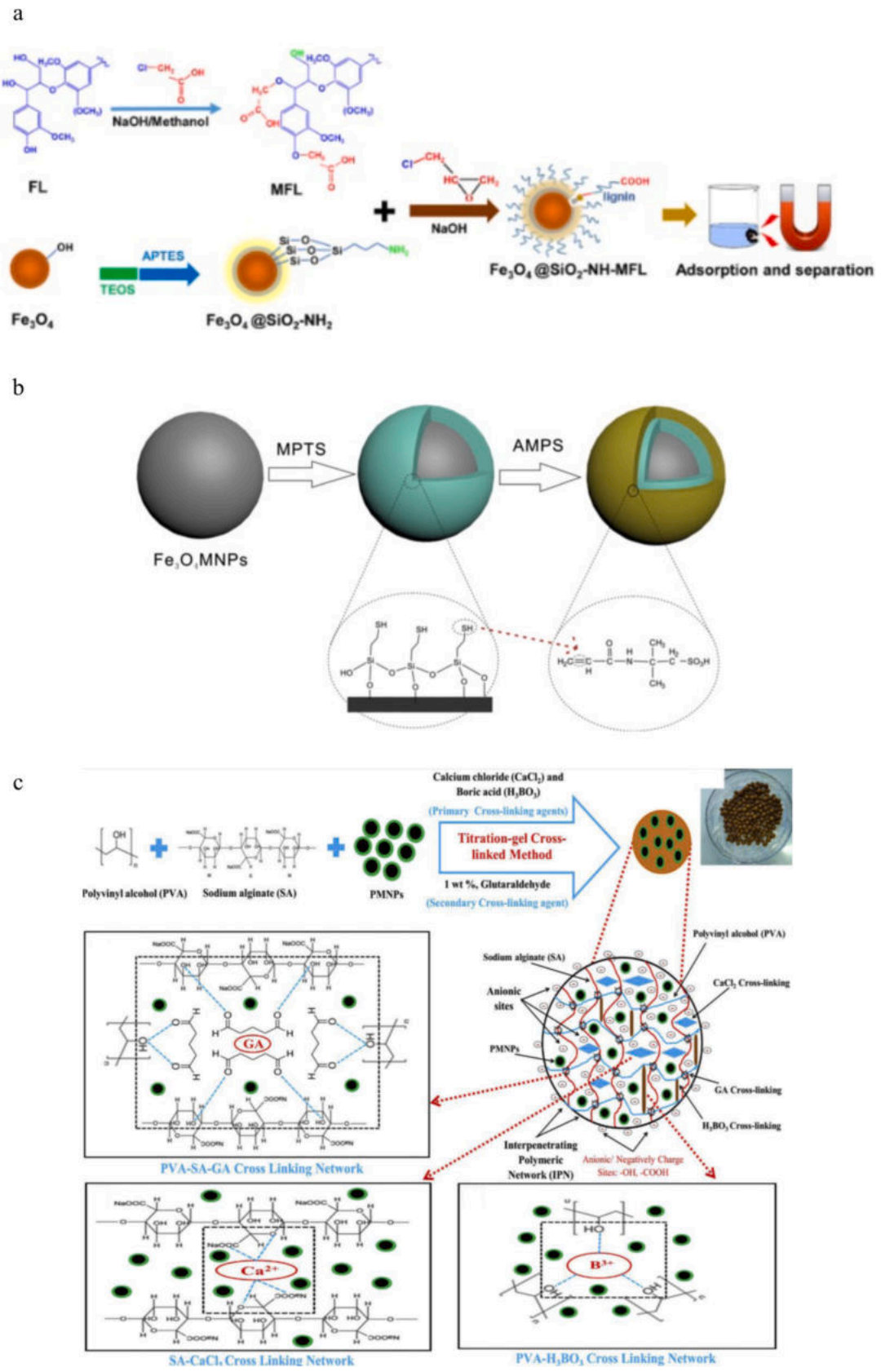

Fig. 4. (a) Schematic process flow diagram illustrating the synthesis of the lignin-based hybrid magnetic nanoparticles [96]. (b) Schematic preparation of sulfo-magnetic nanoparticles [97]. (c) Schematic of the encapsulation of magnetic nanoparticles (MNPs) into bio-magnetic membrane capsules (BMMCs) [98]. Reproduced with permission from [96–98].

yet facile tool that can be applied to recover the adsorbents from effluent by simply applying an external magnetic field. MNPs that having the magnetic responsive behaviour, and as well as, large surface area to volume ratio makes it feasible for the environmental application as the adsorbents for water treatment process. However, colloidal instability of MNPs is the main factor that limits its pollutant removal efficiency. Thus, through modifying the surface properties of MNPs with suitable functional groups that having high affinity towards specific pollutants, not only able to solve the mentioned limitation of MNPs, but also facilitate the pollutant adsorption efficiency and capacity. Surface modification of MNPs also brings an idea for synthesizing a smart material that exhibits multiple functionalities, in which could be used for targeting various types of pollutants to meet the minimum requirement in actual water treatment process. A short summary regarding the usage of functionalized MNPs on the removal of organic, inorganic and microbial pollutants is listed down in Table S4.

2.4. pH-responsive smart materials

pH-responsive is a group of smart materials that can respond to the environment pH variation and result in structural and property changes, such as surface activity, chain conformation, solubility and configuration [105]. They are either polyacids or polybases that are able to donate or accept protons when responding to pH fluctuation. This is due to polyacids having ionizable acid groups such as carboxylic acid (COOH), sulfonic acid (SO_3H) or phosphonic acid (PO_3H_2) along the polymer chains, whereas polybases containing basic groups such as amines (NH_2) in their structural backbone [106]. Ionization of these mentioned functional groups in water or ionizing solvent gives rise to the formation of highly-charged polymeric molecules as shown in Fig. S6 [107]. In general, polyacids behave as anionic polymers at basic conditions, while polybases behave as cationic polymers at acidic conditions. The capability of pH-responsive materials in forming charges polymeric

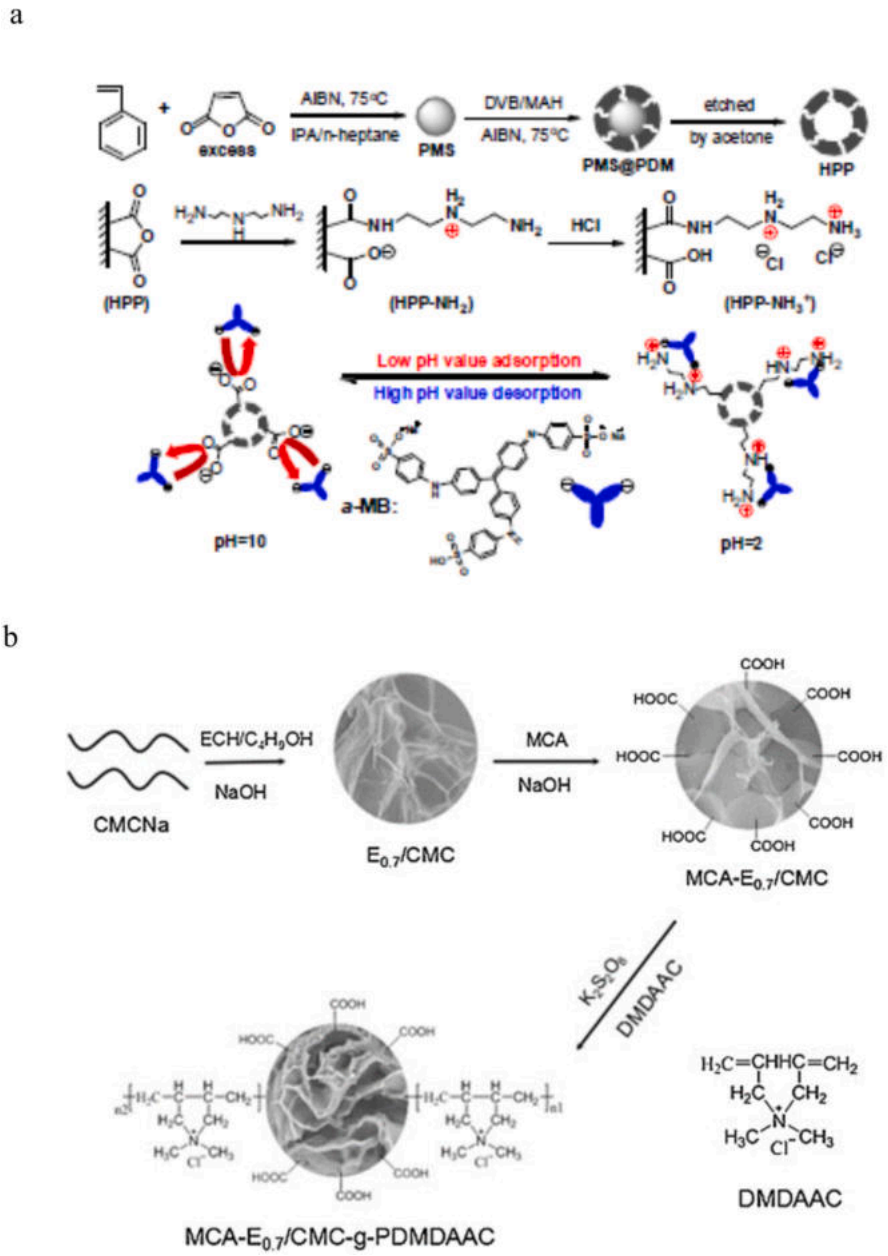

Fig. 5. (a) Schematic illustration of the synthetic route of HPPs-NH_3^+ for the adsorption/desorption of α-MB dye by the HPPs-NH_3^+ [112]. (b) Schematic illustration of MCA-$E_{0.7}$/CMC-g-PDMDAAC microspheres synthesis [116]. Adapted with permission from [112]. Copyright 2016 American Chemical Society. Reproduced with permission from [116].

molecules when respond to pH changes have given them the possibility in removing charged water pollutants. It is necessary to choose either polyacids, polybases or even the combination of both with the right composition in order to achieve the desired water treatment application [105]. There are numerous comprehensive reviews have been published on the classification, characterization, synthesis and applications of pH-responsive materials in the literature [105–111]. However, most of the reviews that have been done are on the biomedical application of pH-responsive materials and only a few papers addressed on environmental application. As a result, a special focus will be given to recent applications of pH-responsive materials in treating organic and inorganic pollutants that are commonly found in polluted water resources.

Over the years, the fabrication of an extra efficient and environmental-friendly pH-responsive adsorbent is the research direction of the scientific community through varying the backbones and doping materials of the adsorbents in order to achieve an ideal organic dyes removal effect for treating the polluted water. For instance, benefiting from the large surface area, perfect mechanical strength and adjustable surface chemistry of hollow polymer particles (HPPs), Yan and the team have designed and synthesized a novel type of ammonium-functionalized hollow polymer particles (HPPs-NH_3^+) that reported highly efficient for the removal of negatively-charged methyl blue α-MB dye in acidic condition [112]. This is due to there was extremely high density of positively-charged ammonium ions present in the cross-linked shell of the as-prepared HPPs-NH_3^+ that were generated from the protonation of the amino groups in the present of HCl as shown in Fig. 5a, which were effective adsorption sites for α-MB dye via strong electrostatic interaction. In greening the 21st century materials, natural polymers have received great concern as the backbone for synthesizing the pH-responsive materials. This is owing to its low cost, inexhaustible source, eco-friendly and biodegradable properties [113,114]. Thus far, natural polymers such as sodium alginate [114], turmeric powder (TP) [115] and carboxymethyl cellulose (CMC) [116] were introduced to derive the pH-responsive adsorbents with improved efficiency on the removal of methylene blue (MB). The carboxyl groups present on the surface of sodium alginate, TP and monochloroacetic acid (MA) treated CMC are the main species that contributed for the adsorption of MB (can refer to Fig. 5b with MCA-$E_{0.7}$/CMC as a reference). This is due to the deprotonation effect of carboxyl groups, forming the carboxylated groups —COO^-, resulting in the electrostatic attraction between the cationic MB and anionic adsorbents. All of the mentioned natural polymer derived pH-responsive adsorbents shared an advantage of ideal MB removal efficiency at neutral pH, enabling in the cost reduction for pH adjusting treatment process. In addition, the effort of Lin et al. [116] by grafting dimethyldiallylammonium chloride (DMDAAC) onto CMC have brought the adsorbent potential for the efficacy adsorption of both cationic MB or anionic orange II (OR II) and methyl orange (MO) dyes through varying the solution pH. The adsorbent combines quaternary ammonium groups (—NR_4^+) from DMDAAC and carboxylic groups (—COOH) from CMC, giving it the advantage of selective adsorption specific dyes based on pH conditions. For instance, the adsorbent shows a positive surface charge at acidic pH due to the protonation of quaternary ammonium groups that facilitates the adsorption of anionic dyes like OR II and MO. Conversely, the adsorbent carries negative surface charges at alkaline pH due to the deprotonation of —COOH to —COO^-, which promotes the adsorption of cationic MB dye. This great contribution has implied the idea of synthesizing a novel adsorbent with multi-pollutants removal possibility to address the real-life water treatment application.

By referring to the works of Lu [114] and Kubra [115], pH-responsive swelling ratio of the adsorbents play a vital role in the adsorption of dyes, whereby higher degrees of swelling could favor the occurrence of hydrogen bonding in between the hydrophilic functional groups present on the adsorbents and the dyes, leading to high dye uptake capacity. Moreover, most of the dye's adsorption approach taken place in aqueous environment, in which the water molecules could weaken the polar affinity between the adsorbents and the dyes [117]. In this consideration, pH-responsive natural polymer-based hydrogels with magnificent swelling ratio and large water retention capability shall possess great dyes removal efficiency and eco-friendly properties. For instance, an environmentally friendly pH-responsive superabsorbent hydrogel has been synthesized by free radical graft *co*-polymerization of sodium acrylate (NaAc) and acrylamide (AM) on banana pseudo-stem carboxymethyl cellulose (BPCMC) for the removal of cationic MB dye [118]. In the same vein, Thakur and the team have synthesized poly-acrylic acid grafted sodium alginate (SA-cl-PAA) based hydrogel that reported excellent performance in the removal of cationic victoria blue (VB) and rhodamine 6G (RG6) dyes [119]. Moreover, poly(*N*, *N*-dimethyl acrylamide) grafted locust bean gum (LBG) hydrogel (LBG-cl-Poly(DMAAm)) prepared via free radical in situ polymerization was found highly efficient in removing water-soluble cationic dye Brilliant green (BG) [120]. The superior cationic dyes removal efficiency for the mentioned natural polymer-based hydrogels are due to the COOH groups on the backbone of hydrogels ionize to form COO^- groups at specific pH range, in which the electrostatic repulsion occurs among COO^- groups lead to expansion of the hydrogels and enhancement in swelling capacity that promote hydrogen bonding between the hydrogels and the dyes. Besides, the anionic COO^- groups also further contribute for the adsorption of cationic dyes via electrostatic interaction. By contrast, for the adsorption of anionic MO dye, not only the swelling effect of hydrogel, but also the amino groups present in the hydrogels of poly(acrylamide-*co*-diallyldimethylammonium chloride) grafted salecan [117] and 2-(dimethylamino) ethyl methacrylate (DMAEMA) grafted CMC [121] that are protonated at low pH to form NH_3^+ ionized groups, which further promote for the effective anionic MO dye adsorption.

For tackling the inorganic heavy metal pollutant issues in water source, immense efforts have done by the scientific community in fabricating novel pH-responsive adsorbents with the aim to achieve optimal heavy metal removal performance that is practicable in real life application. For instance, glutaraldehyde (GA) cross-linked sodium alginate (SA) [114], amide-based covalent organic frameworks (COFs) [122], *N*,*N*′di(3-carboxysalicylidene)-3,4-diamino-5-hydroxypyrazole (DSDH) anchored mesoporous inorganic silica [123] and *N*,*N*(octane-1,8-diylidene)di(2-hydroxy-3,5-dimethylaniline) (DHDM) anchored mesoporous silica [124] adsorbents have shown effective in the removal of Fe^{3+}, Pb^{2+}, Co^{2+} and Cu^{2+} ions respectively. Furthermore, it is honoured to mention the work reported by D'Haluin et al. where a chemically modified cellulose filter paper with ethylenediaminetetraacetic acid (EDTA) had shown more than 90 % of removal efficiency against Ag^+, Pb^{2+}, Cd^{2+}, Ni^{2+}, Zn^{2+}, Sn^{2+} and Cu^{2+} [125]. The fabricated adsorbents shared a similarity of containing either anchored ligand or chelating agent that having free lone pair electrons on O or N atoms which can form stable coordinate bonds with heavy metal ions as shown in Fig. S7 regarding the multi-coordination of Pb^{2+} by COFs as the example. Meanwhile, the functional groups present in each of the adsorbents mentioned (mainly amino groups) have given rise pH-responsive property to the adsorbents, where deprotonation of the amino groups at alkali condition have given the adsorbents with negatively-charged surface that are beneficial for the adsorption of positively-charged heavy metals via electrostatic interaction. Liu and his coworkers, for instance, have synthesized an eco-friendly straw-based adsorbent that modified through grafting with acrylamide (AM) and citric acid (CA) reported effective in the adsorption of both anionic $Cr_2O_7^{2-}$ and cationic Cu^{2+} by varying the solution pH [126]. A summary of reported pH responsive smart materials for water treatment application is shown in Table S5.

2.5. Multi-stimuli responsive smart materials

Thus far, abundant of adsorbents or smart materials applied mainly in water treatment application and respond to single stimulus have been

discussed. However, it is always interesting to develop materials that are capable of responding to two, three or even more stimuli simultaneously. As this will provide extra and diverse functionalities for the adsorbents to possess excellent pollutant removal efficiency, multiple pollutants removal possibility, great recyclability and long-term stability. To the best of our knowledge, there are scarcely reviews have been done on the multi-stimuli responsive smart materials that used in environmental and water treatment applications. Hence, a special focus is given to the enhancement removal efficiency of smart materials possess multiple stimuli responsive properties towards organic, inorganic and microbial pollutants. The combination of stimuli discussed in this section include but not limited to magnetic, light, temperature and pH, which are the most common and well-studied stimuli by our research community with magnetic as the core for each group of multi-stimuli responsive materials because of their facile separation, easy functionality and relatively inexpensive.

2.5.1. *Magnetic and light responsive*

Advancing to the green chemistry concept, the recent developed strategies are focusing on the fabrication of sunlight and/or visible light-based groups of novel modified photocatalysts carrying magnetic property for water remediation application. For instance, a composite photocatalyst based TiO_2 and magnetic Matérial Institute Lavoisier (MIL-101 (Cr), one of metal-organic frameworks (MOFs)) was successfully synthesized by Zhang's group [127] via a facile hydrothermal in situ growth method as shown in Fig. 6a. The composite exhibited remarkable removal efficiency to bisphenol-F (BPF) and acid red 1 (AR1) dye under the irradiation of visible light. This is owing to the enormous surface areas and ultrahigh porosity of MIL-101 (Cr) that significantly enhance the dye adsorption which is in favor of photocatalytic degradation between the radicals and the adhering organic dyes. Besides, MIL-101 (Cr) can aid in trapping the photoelectrons, resulting in preventing the recombination of electron-hole pairs, leading further to an obvious improvement on photocatalytic activity [127]. In addition, Fe_3O_4 not only plays a role in the convenience magnetic separation, but also provides intensive visible light absorption with the formation of Fe-intra-gap states as presented in Fig. 6b, in which the Fe dopants introduce additional energetic levels in the band gap of the doped TiO_2 that allows the reduction and narrower of the optical absorption edge [127,128]. In another approaches, by introducing additional semiconductors, such as $CoMoO_4$ [129] and POMs [128] into the combination of iron oxide (magnetic counterpart) and TiO_2 (light-responsive photocatalyst) forming $Fe_3O_4/TiO_2/CoMoO_4$ and TiO_2/FeOx/POM, resulted in the enhancement visible light absorption and outstanding photocatalytic degradation towards organic dyes (methylene blue (MB), methyl orange (MO), congo red (CR) and Rhodamine B (RhB)) and 2,4-dichlorophenol (2,4-DCP). The formation of a semiconductor-semiconductor heterojunction reduces the band gap energy (as shown in Fig. 6c) and decreases the rate of photo-generated carriers recombination by yielding long-lived electron-hole pairs, leading to the adsorption intensity showed an increment in the visible light region and significant improvement of the photocatalytic activity [128,129]. Additionally, the iron oxide magnetic counterpart acts as an electron reservoir for the exited electrons generated by the photocatalyst components, promoting efficient charge separation that significantly enhances the photocatalytic activity of the composites. Moreover, its superparamagnetic behaviour facilitates simple and rapid magnetic separation, ensuring ease of recovery and recyclability.

Alternatively, POMs have received much attention as an excellent photocatalyst and light-responsive moiety due to its fascinating

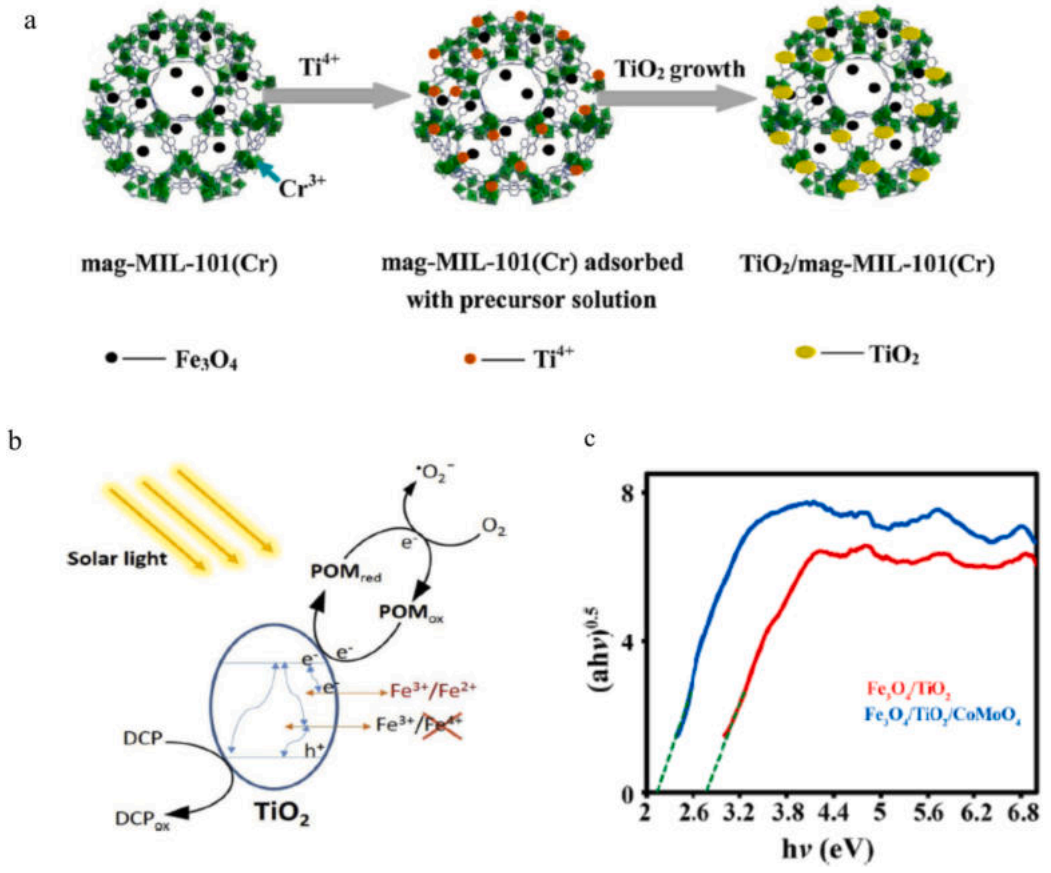

Fig. 6. (a) Schematic diagram of TiO_2/mag-MIL-101 (Cr) synthesis [127]. (b) Schematic diagram of the formation of Fe-intra-gap states [128]. (c) Plots for the determination of band gap of Fe_3O_4/TiO_2 and $Fe_3O_4/TiO_2/CoMoO_4$ [129]. Reproduced with permission from [127–129].

semiconductor and optical properties as discussed in Section 2.2. The incorporation of POMs into the magnetic particles are current emerging trend in forming the magnetic and light dual stimuli responsive smart materials. As an instance, a core-shell composite consists of Fe_3O_4 as the core and POMs as the shell with silver nanoparticles as the noble metal doping was synthesized via sonochemical [130] and impregnation [131], forming Fe_3O_4/Ag/POMs and Fe_3O_4@SiO_2@mSiO_2-PW_{12}/Ag respectively, reported more than 96 % removal efficiency for the photocatalytic degradation of organic dyes. Ag nanoparticles, the noble metal, is the most common and magnificent supplement for photocatalysts, beneficial from its strong surface plasmon resonance (SPR) and high electron trapping performance, in which can be used to modify the visible light absorption and improve the separation of photo-generated charges that subsequently enhance the photocatalytic activity of the composites [130,131]. Typically, an additional supporting layer, such as SiO_2 [131], Al_2O_3 [132] (photo-catalytically inefficient) or ZnO [133] (photo-catalytically efficient) is utilized for the immobilization of POMs and existed in between the magnetic core and POMs, in order to prevent the undesirable movement of photo-generated charges from the active photocatalyst to the magnetic core, leading to the diminish of photocatalytic activity. The photo-catalytic inefficient SiO_2 and Al_2O_3 provide high surface area for the immobilization of more POMs species, while the photo-catalytic efficient ZnO plays the role in the formation of semiconductor-POMs heterojunction gives a synergistically positive effect for photocatalytic performance [132,133].

For the elimination of heavy metals, Wu and coworkers [131] were successfully prepared the novel composite, Fe_3O_4@SiO_2@mSiO_2-PW_{12}/Ag reported as high as 91.2 % photoreduction of Cr (VI). In a different approach, Li's group [134] synthesized a sandwich structured of Fe_3O_4/Ag/m(TiO_2-ZrO_2) magnetic photocatalyst showed great reduction efficiency of Cr (VI) achieved 98.4 % in 30 min. Both of the researchers perfectly utilized the advantages of noble metal Ag, which the intense SPR effect of Ag can broaden the light response range and Ag can act as an electron trap thereby facilitating the separation of photo-generated electron-hole pairs, consequently enhancing the photocatalytic performance. It is worth to mention the effort done by Li's group [134], where another sandwich nanospheres with different fabrication sequence were synthesized by placing Ag nanoparticles as outermost shell (as shown in Fig. S8) producing Fe_3O_4/m(TiO_2-ZrO_2)/Ag to investigate the effect of structural sequence on the reduction of Cr (VI). Notably, the reduction efficiency of Fe_3O_4/Ag/m(TiO_2-ZrO_2) was 1.6 times higher than Fe_3O_4/m(TiO_2-ZrO_2)/Ag, because of the obstruction of outermost Ag nanoparticles limit the active sites for the contact between Cr (VI) and the nanospheres [134]. In both studies, the mesoporous structures of the mSiO_2 and m(TiO_2-ZrO_2) shells serve as supporting layers that provide abundant specific surface area, facilitating the loading of more active species. This enhances light-harvesting efficiency and promotes photocatalytic reactions. Similarly, both synthesized composites experienced unavoidable reduction in magnetic saturation due to sequential coating of non-magnetic materials. Despite this, the composites retained their superparamagnetic properties, ensuring efficient recovery with an external magnetic field.

The photocatalytic bacterial inactivation performance of magnetic photocatalyst can be visualized in the work of He and the team [135], a solar-driven reduced-graphene-oxide/Fe,N-TiO_2/Fe_3O_4@SiO_2 (RGOFeNTFS) was developed to examine the different responses of photocatalytic disinfection towards gram-negative (*E. coli* and *S. typhimurium*) and gram-positive (*E. faecalis*) bacteria. The co-doped TiO_2 with Fe and N narrows the bandgap, enhancing the photocatalytic activity of the material under visible-light that improves the solar-light-driven utility of the composite. While reduced graphene oxide (RGO) enhances the charge separation by migrating the photocatalytically generated electrons to the composite surface. The results indicated that the gram-positive *E. faecalis* bacterium appears to be more susceptible to the photocatalytic reaction (highest reduction in the cells among all three bacteria), due to its single phospholipid bilayers membrane present in the gram-positive *E. faecalis* is less resistant to photocatalytic disinfection than gram-negative bacteria that having dual phospholipid bilayers [135]. On top of that, as a potential technique for real scenario sewage or water treatment, photocatalytic disinfection using RGOFeNTFS in mixed bacteria culture was studied, which disinfection of all three bacteria occur simultaneously under simulated solar irradiation, but gram-negative *S. typhimurium* reported slightly higher bacterial density reduction. This is attributed to the degree of interactions between the RGOFeNTFS and the individual bacteria, whereby *S. typhimurium* has a more negative surface charge providing the highest adhesion to the positively-charged RGOFeNTFS [135]. Another excellent photocatalytic disinfection by POMs-based magnetic nanocomposite can be witnessed in the study of Khudhair's group [136]. A new hybrid nanocomposite photocatalyst was developed via the immobilization of phosphotungstic acid (POMs) on Fe@ZnO, resulting Fe@ZnO/PW could completely inactivate 10^7 cfu/mL of *E. coli* after 2 h of visible light irradiation. The semiconductor composites (ZnO/PW) work on photocatalytic bacterial inactivation, while magnetic material moiety (Fe) provides a facile method to separate and recover the photocatalysts. A summary and comparison of reported magnetic and light responsive smart materials for water remediation application is presented in Table 1.

2.5.2. Magnetic and pH

Dual responsiveness towards magnetic and pH stimuli have been demonstrated by Yao and coworkers [138], a modified magnetic graphene oxide/poly (NVI-*co*-AA) (MGO/PNA) was synthesized by random copolymerization of negatively-charged acrylic acid (AA) and positively-charged NVI in the presence of graphene oxide (GO) in aqueous medium for the removal of organic dyes (methyl violet (MV), methylene blue (MB), tartrazine (TZ), amaranth (AR)). This study well illustrated the utilization of both polyacid and polybase in single entity, in which the deprotonation and protonation of the ionizable acid and basic groups when respond to pH fluctuation give rise to the formation of highly-charged molecules that can interact with charged pollutants such as organic dyes and heavy metals via electrostatic interaction [138–140]. At low pH, the imidazole-N groups in the hydrogel are protonated and showing positive charges that are suitable for the adsorption of anionic dyes (TZ and AR), while the carboxyl groups of PAA segment are deprotonated in high pH medium and giving negative charges which the cationic dyes (MV and MB) are strongly adsorbed by electrostatic attraction as shown in Fig. S9. The introduction of Fe_3O_4 nanoparticles into the hydrogel system could not only improve the recyclability of materials, besides the interaction between Fe_3O_4 and GO sheets can effectively prevent the redeposition of GO and the agglomeration of Fe_3O_4 particles. Thus, the addition of Fe_3O_4 improves the colloidal stability, surface area of the composite and the adsorption capacity of the hydrogel to some extent [138]. Keeping in mind the principles of green chemistry, Lee and associates [90] fabricated magnetic multi-walled carbon nanotubes (n-MMWCNTs) via a facile and solvent-free direct doping method for the removal of MB. The result reported a corresponding enhancement on the removal efficiency of MB from 41.49 % to 89.77 % when the solution pH was increased from 3 to 11. At alkaline medium condition, the surface charge of n-MMWCNTs became more negative in light of higher deprotonation of hydroxyl groups in Fe_3O_4 and carboxyl groups in MWCNTs, providing stronger electrostatic attraction to the cationic MB dye molecules [90].

In terms of the effort in eliminating toxic heavy metal ions, magnetic biochar [141], magnetic graphene oxide (MGO) [142] and functionalized lignin-based magnetic adsorbents (L1@MNP) [143] were prepared for the removal of Cr (VI), Cr (III). Cu (II), Zn (II), Ni (II) and Pb (II). The abundance of active functional groups (carboxyl and hydroxyl) in the molecular structures of biochar, graphene oxide and lignin make them as an excellent adsorbent for removing toxic metal ions from water. Most of the heavy metal ions (Cr (III). Cu (II), Zn (II), Ni (II) and Pb (II)) exhibiting positive charges in the aqueous solution, hence the removal efficiency enhanced significantly as the increment of pH, due to the

Table 1
Summary and comparison of reported magnetic and light responsive smart materials for water remediation application.

Magnetic and light responsive compounds	Fabrication method	Pollutants	Surface area (m^2/g)	Pore volume (cm^3/g)	Band gap energy (eV)	Operational conditions	Removal efficiency (%)	Reusability (cycle)	References
TiO_2/mag-MIL-101 (Cr)	Facile hydrothermal in situ growth	Bisphenol-F (BPF), acid red 1 (AR1)	–	–	1.61	Photocatalyst dosage: 20 mg/40 mL; Dye concentration: 20 ppm; Temperature: 25 °C; 500 W xenon lamp equipped with UV-cutoff filter and placed 15 cm away from the suspension	90	5	[127]
TiO_2/Fe_3O_4/Graphene oxide	Facile hydrolysis	Methylene blue (MB)	–	–	2.7	Photocatalyst dosage: 0.02 g/200 mL; Dye concentration: 10ppm; Temperature: 25 °C; pH: 11; 4 drops of hydrogen peroxide; 500 W halogen lamp as the visible light source	76	4	[137]
Fe_3O_4/TiO_2/$CoMoO_4$	Sonication	Methylene blue (MB), methyl orange (MO), congo red (CR), Rhodamine B (RhB)	141.7	0.543	2.18	Photocatalyst dosage: 0.04 g/ 50mL; Dye concentration: 20ppm; Temperature: 25 °C; 30 µL of 30 % hydrogen peroxide added; sunlight irradiation	MB: 99.9 MO: 98.4 CR: 96 RhB: 98.7	5	[129]
Fe_3O_4/Ag/POMs	Sonochemical	Methylene blue (MB)	–	–	–	Photocatalyst dosage: 0.005 g/30 mL; Dye concentration: 15 ppm; Temperature: 25 °C; 300 W xenon lamp equipped with filter to match the visible light and placed 10 cm away from the reaction beaker	98.7	6	[130]
Fe_3O_4@SiO_2@mSiO_2-PW_{12}/Ag	Impregnation	Methyl orange (MO), Cr (VI)	172	0.15	–	Photocatalyst dosage: 0.04 g/40 mL for MO, 0.03 g/ 30 mL for Cr (VI); Dye concentration: 20 ppm; Cr (VI) concentration: 500 ppm; Temperature: 25 °C; pH: 2; 300 W xenon lamp as the simulated sunlight	MO: 100 Cr (VI): 91.2	5	[131]
Fe_3O_4@Al_2O_3-PMo	Impregnation	Cibacron Brilliant Yellow 3G-P (CBY)	54.6	0.231	2.22	Photocatalyst dosage: 1 g/L; Dye concentration: 40 ppm; H_2O_2: CBY molar ratio: 0.2; pH: 7.2; Air flowrate: 0.15 LPM; 8 W UV lamp as the visible light source	83.5	5	[132]
Fe_3O_4@ZnO/PMo	Impregnation	Methyl orange (MO)	46.2	0.156	–	Photocatalyst dosage: 0.04 g/ 50mL; Dye concentration: 40 ppm; pH: 7.1; 2×20 W white LED lamp as the visible light source	92.3	6	[133]

(*continued on next page*)

Table 1 (*continued*)

Magnetic and light responsive compounds	Fabrication method	Pollutants	Surface area (m^2/g)	Pore volume (cm^3/g)	Band gap energy (eV)	Operational conditions	Removal efficiency (%)	Reusability (cycle)	References
TiO_2/FeOx/POM	Impregnation	2,4-dichlorophenol (2,4-DCP)	48.31	–	2.65	Photocatalyst dosage: 0.025 g/50 mL; 2,4-DCP concentration: 10 ppm; pH: 5.0; solar light irradiation	76.0	5	[128]
Fe_3O_4/Ag/m(TiO_2-ZrO_2)	Sol-gel	Cr (VI)	324.5	–	1.66	Photocatalyst dosage: 0.004 g/20 mL; Cr (VI) concentration: 10 ppm; pH: 3; 350 W Hg lamp situated at 10 cm away from the solution surface	98.4	5	[134]
Reduced-graphene-oxide/Fe,N-TiO_2/Fe_3O_4@SiO_2 (RGOFeNTFS)	Sol-gel	*Escherichia coli* (*E. coli*), *Salmonella typhimurium* (*S. typhimurium*), *Enterococcus faecalis* (*E. faecalis*)	–	–	2.76	Photocatalyst dosage: 1 g/L; Bacterial concentration: ~10^4 cfu/mL; 300 W xenon light equipped with filter to stimulate solar irradiation	*E. coli*: 4.2-log *S. typhimurium*: 4.1-log *E. faecalis*: 4.5-log	–	[135]
Fe@ZnO/PW	Impregnation	*Escherichia coli* (*E. coli*)	63.5	0.156	2.23	Photocatalyst dosage: 0.8 g/L; *E. coli* concentration: 0.95 * 10^7 cfu/mL; Temperature: 25 °C; 8 W white LED lamps as the visible light source	100	6	[136]

deprotonation of the functional groups and the adsorbents surface became more negatively-charged which were favourable for attracting positive heavy metal ions. Conversely, Cr (VI) exists in the forms of $HCrO_4^-$, CrO_4^{2-} and $Cr_2O_7^{2-}$, hence the prepared modified biochar adsorbents reported maximum removal efficiency at low pH because of the protonated surface functional groups to generate electrostatic attraction between the positively-charged adsorbents and negatively-charged metal ions [141]. Moreover, gaining from the presence of magnetic cores in the network structure expedites the facile and quick recovery of the adsorbents after the adsorption process.

In addition, Hinsene and the team [144] successfully synthesized a ternary recyclable rice husk biochar doped with deep eutectic solvent (DES) and Fe_3O_4/ZnO nanoparticles (Fe_3O_4-ZnO/RBC-DES) for the removal of Cr (VI), Pb (II), and diclofenac sodium (DCF). The DES used was composed of choline chloride (ChCl) as hydrogen bond acceptor (HBA) and urea as hydrogen bond donor (HBD) at a 1:2 M ratio. The composite with higher molar ratio of Fe_3O_4 and ZnO, denoted as FZRBC-DES15 demonstrated exceptional removal efficiencies of 95.1 % for Cr (VI), ~100 % for Pb (II), and 69.2 % for DCF, attributed to the synergistic contributions of its modification components. For instance, the surface functional groups of FZRBC-DES15 contain COO^-, Si—O— and —OH from biochar, —NH_2 from DES, and Fe—O and Zn—O from metal oxide nanocomposite, enhance adsorption through improved surface activity by providing more active adsorption sites. At low pH, protonation of these functional groups provides a cationic surface that attracts negatively charged Cr (VI) ions via electrostatic interactions. Additionally, both Fe_3O_4 and ZnO nanoparticles act as reducing agents facilitate the reduction of Cr (VI) to Cr (III). At higher pH, deprotonation of the surface functional groups take place, leading to more Pb (II) adsorption onto the surface of the nanocomposite, while ion exchange involving Na^+, K^+, Ca^{2+}, Zn^{2+}, and Fe^{2+} cations further supports Cr (III) and Pb (II) adsorption. Functional groups such as COOH, C—OH, and —NH_2 promote surface complexation and coordination bonding with Cr (VI) and Pb (II), subsequently aiding the adsorption. DCF removal is dominated by hydrogen bonding interactions between DCF's —OH and —NH_2 groups and the composite's carboxylic, phenolic, —OH, —NH_2, and π-π stacking interactions. Additionally, Fe_3O_4 offers magnetic properties that enable easy separation and recyclability. This study highlights the advantages of deep eutectic solvents (DESs) in enhancing the surface functionalities of the nanocomposite, introducing additional active sites that improve the adsorption performance for metal ions and organic pharmaceutical pollutant through interactions such as ion exchange, hydrogen bonding, and the formation of coordination complexes. DESs mimic the properties of ionic liquids (ILs), but outweigh them in terms of low cost, simple preparation, environmental friendliness, and tunable functionalities [145]. These characteristics make DESs one of the ideal candidates for the development of advanced adsorbents that are in line with the green chemistry principles, while achieving high removal efficiencies for a broad range of water pollutants. More and more future research should focus on actively designing DES-based adsorbents to address current persistent challenges in water treatment applications.

Ain and co-workers [142] further utilized the synthesized MGO to demonstrate its antibacterial activity against *Escherichia coli* (*E. coli*), *Yersina ruckeri* (*Y. ruckeri*) and *Antobacter agglomerans* (*A. agglomerans*). An excellent sterilization effectiveness of 98.787 %, 97.150 % and 97.689 % were reported towards *E. coli*, *Y. ruckeri* and *A. agglomerans*. Overall, the results ascertained the prominent antimicrobial property of the synthesized magnetic and pH responsive MGO towards different bacterial strains. However, there is lacking of tedious study regarding the antimicrobial action and the pH varying effect on the antimicrobial efficiency. In fact, most of the researches nowadays are conducted for the removal of organic dyes, and very few studies are available for the adsorption or removal of microbial contaminants. Further exploration on the removal of microbial pollutant is necessary to attain a comprehensive antimicrobial response, meeting the practical demands of wastewater treatment. The magnetic and pH responsive smart materials

are summarized in Table 2.

2.5.3. Magnetic and thermal

Upon the introduction of thermal responsive material PNIPAM onto magnetic particles give a more comprehensive adsorbent with rapid separation property and mechanistic function in controlling the uptake and release of pollutants under the effect of temperature change. Zhou and co-workers [146] designed a magnetic hydrogel with interpenetrating network (IPN) by crosslinking NIPAM via free radical polymerization in the presence of chitosan and Fe_3O_4, forming the magnetic poly(N-isopropylacrylamide)/chitosan hydrogel to evaluate the adsorptive performance for emerging contaminants hydrophilic sulfamethoxazole (SMZ) and hydrophobic bisphenol A (BPA). The effect of temperature on the adsorption of SMZ was not significant, due to the main adsorption driving force was electrostatic attraction between the positively-charged amino groups of chitosan and negatively-charged SMZ (Fig. 7a), which was less likely to be affected by temperature. On the flip side, increment in the adsorption temperature greatly promoted the adsorption capacity of BPA, because of the phase transition of PNIPAM changed from hydrophilic to hydrophobic when the temperature increased from 25 °C to 35 °C, which enhanced the hydrophobic interaction between the magnetic hydrogel and BPA, resulting in a substantial increment in the adsorption capacity [146]. The uptake and release mechanistic action of PNIPAM when responds to temperature changes was also demonstrated in the removal of Sudan red dye by the magnetic and thermal dual-sensitive nanoparticles based on silica coated nano-scale zero valent iron with NIPAM and methyl 3,3-dimethylacrylate (DMMA) (Fe@p(NIPAM-co-DMMA)) [147]. The magnetism property of the composites was utilized for quick and effective isolation of the adsorbents from aqueous solution, while the thermal-sensitive of coated PNIPAM was used for the adsorption and desorption of dye molecules. This can be achieved through switching the medium temperature between 25 °C and 35 °C, in which the adsorption was enhanced at 35 °C that attributed to the enrichment of hydrophobic interaction between the coated PNIPAM and Sudan red dye molecules. Conversely, desorption was accomplished at 25 °C, where the PNIPAM polymer chains turned more hydrophilic and weaken the interaction between PNIPAM and Sudan red dyes.

The phase transition characteristic of magnetic and thermal-responsive materials was employed for the recovery or removal of heavy metal ions as well. Chen and the group [149] successfully developed a magneto-thermo-responsive composite hydrogel through *co*-polymerized acrylic acid (AA) with PNIPAM onto the silica-coated magnetic nanoparticles to form (PNIPAM-co-AA)-silica-PVP-MNPs for the removal of Cr^{3+} ions. The adsorption of Cr^{3+} are chelated by multidentates via different interactions including electrostatic interaction, hydrogen bonding as well as covalent bonds on the hydrogel surfaces bound by the carboxylates (—COO^-) of the AA moiety and amides of PNIPAM that are prominent electron-donating groups to form metal-ligand surface complexes. At room temperature (below the LCST of PNIPAM), the hydrogel is hydrophilic and allowing Cr^{3+} ions to diffuse into the hydrogel matrix for adsorption. At higher temperatures (50 °C, above the LCST of PNIPAM), the desorption of Cr^{3+} happened, signified the release of physisorbed Cr^{3+} ions back to the bulk solution. However, this phenomenon is contrary at lower initial concentrations of Cr^{3+} (20 to 50 mg/L), where continual uptake of Cr^{3+} is observed when temperature rose from room temperature to 50 °C. This is due to heating-driven hydrolysis of Cr^{3+} ions converted coordinated water molecules anchored around Cr^{3+} centre into hydroxyl groups. The hydrolysed Cr^{3+} bearing hydroxyl groups exhibit higher affinity towards the binding groups of hydrogels through stable hydrogen bonding and precipitated onto the hydrogel surface. Another interesting finding revealed that the adsorbed Cr^{3+} ions on the AA *co*-polymerized hydrogels was mainly aggregated on the surface, creating a bridging effect that induced hydrogel agglomeration, which in turn enhanced their magneto-responsiveness. In another study, Tomonaga and co-workers [148] recorded similar findings with the enhancement adsorption of Cu^{2+} ions by poly(NIPAM-*co*-AA)/silica-coated MNP composite at 60 °C when compared to 10 °C. In brief, when the medium temperature is above the LCST, the hydrophobic aggregation of the copolymer reduces the distance between carboxyl groups of the composite and Cu^{2+} ions, which chelating can be formed more easily (Fig. 7b). Vice versa, at temperature lower than the LCST, the increase of the hydrophilicity leads to the expansion on the average distance between carboxyl groups and the heavy metal ions, resulted decrement in the number of adsorption sites and lower adsorption capacity [148].

For the separation of microbial pollutants, Zheng's group [150] established the magnetic and thermal-responsive polymer brushes by surface-initiated atom transfer radical polymerization of N-isopropylacrylamide (NIPAm) and allyl glycidyl ether (AGE), followed by a reaction of epoxy groups, and incorporation of magnetic particles and 3,5-difluoro-4-formylphenyboronic acid (DFFPBA), forming Fe_3O_4@poly(NIPAm-*co*-AGE)@DFFPBA illustrated controllable binding of cis-diol-containing bacteria species (*Salmonella* spp. and *S. aureus*) by altering the solution temperature. The multiple boronic acid ligands in DFFPBA contribute to strong affinity binding with cis-diol-containing bacteria. Although the incorporation of DFFPBA also provides pH-responsive property to the copolymer brush, however, the neutral pH is crucial for the demand of bacterial bioactivity and recorded the highest bacteria binding to Fe_3O_4@poly(NIPAm-co-AGE)@DFFPBA, which makes this functionality less significance in this study. Hence, only magnetic and thermal-responsive properties are considered. The bacterial bindings were favourable at 20 °C, but the binding of *Salmonella* spp. and *S. aureus* by Fe_3O_4@poly(NIPAm-co-AGE)@DFFPBA dropped noticeably to 46.64×10^6 cfu/mg and 7.33×10^6 cfu/mg, respectively, indicating that the higher temperature certainly induced the desorption of bacterial strains. The Fe_3O_4 nanoparticles ensure magnetic separation, makes the separation of bacteria more convenient and efficient. Table 3 summarizes the adsorption operational conditions and performance of reported magnetic and thermal responsive smart materials for water treatment application.

2.5.4. Triple-stimuli responsive materials

A novel magnetic, light and thermal responsive photocatalyst, zinc-tetracarboxyl-phthalocyanine-g-Fe_3O_4@SiO_2@TiO_2-g-PNIPAM was synthesized by C. Liu et al. for the removal of RhB and MB dyes [152]. This work reveals the advancement of multi-stimuli responsive smart materials by using the magnetic photocatalyst (Fe_3O_4@SiO_2@TiO_2) as base and further modified with zinc-tetracarboxyl-phthalocyanine (ZnTcPc) and PNIPAM. ZnTcPc is a kind of common dye used to sensitize TiO_2 for extending the photocatalyst light response to visible region. While PNIPAM helps in improving the dispersion stability of the composite in aqueous dye solution (below LCST of PNIPAM) and facilitating regeneration (above LCST of PNIPAM). The composite synthesized reported as high as 91.8 % and 87.7 % photodegradation efficiency of RhB and MB dyes respectively, under visible light irradiation. Both magnetic and thermal responsive properties provide synergistic effect on the recoverability and reusability of the composite, with only 9.6 % reduction noticed in the degradation rate of RhB after 4 cycles of reused.

In a similar approach, Wang and the group demonstrated the magnificent multiple types of pollutants removal possibility, including the adsorption of cationic basic fuchsin (BF) dye, photodegradation of antibiotics ciprofloxacin (CIP) and norfloxacin (NFX), and antibacterial activity against *E. coli* under dark condition by the synthesized iron (II, III) oxide/poly (N-isopropylacrylamide-*co*-methacrylic acid)/silver-titanium dioxide (Fe_3O_4/P(NIPAM-co-MAA)/Ag-TiO_2) nanocomposite [153]. Each smart responsive moieties play its role contributes to the excellent functionalities of this nanocomposite, for instance, the presence of carboxylic groups on P(NIPAM-co-MAA) aided in the adsorption of cationic BF dye, while Ag-TiO_2 gives the composite

Table 2
Summary of reported magnetic and pH responsive smart materials for water remediation application.

Magnetic and pH responsive compounds	Fabrication method	Pollutants	Surface area (m^2/g)	Pore volume (cm^3/g)	Operational conditions	Removal efficiency (%)	Adsorption capacity (mg/g)	Reusability (cycle)	References
MGO/PNA	Random copolymerization	Methyl violet (MV), methylene blue (MB), tartrazine (TZ), amaranth (AR)	–	–	Adsorbent dosage: 10 mg/10 mL; pH: 2 (for anionic dyes), 12 (for cationic dyes)	MV: ~83 MB: ~93 TZ: ~90 AR: ~90	MV: 609.8 MB: 625.0 TZ: 613.5 AR: 609.8	5	[138]
n-MMWCNTs	Solvent-free direct doping	Methylene blue (MB)	168.88	–	Adsorbent dosage: 45 mg/20 mL; Dye concentration: 100 ppm; pH: 11; contact time: 3 h	89.77	20.37	–	[90]
Fe_3O_4@SiO_2@NH_2	Post-synthesis grafting	Methyl red (MR)	–	–	Adsorbent dosage: 0.5 g/L; Dye concentration: 100 ppm; pH: 5.24; contact time: 3 h; mixing speed: 300 rpm	51.64	125	–	[139]
m-Cs-PVA/FA	Crosslinking	Reactive Orange 16 (RO16)	0.5643	0.00138	Adsorbent dosage: 0.06 g/100 mL; Dye concentration: 20–200 ppm; pH: 4; contact time: 5-30 min; Temperature: 30 °C	90.3	123.8	–	[140]
Magnetic biochar	Co-precipitation	Cr (VI), acid orange 7 (AO7)	99.83	–	Adsorbent dosage: 0.5 g/L; Dye and metal ion concentration: 10 ppm; pH: 2; contact time: 180 min; mixing speed: 80 rpm	Cr (VI): 90 AO7: 90	Cr (VI): 80.96 AO7: 64.40	5	[141]
Magnetic graphene oxide (MGO)	Co-precipitation	Pb (II), Cr (III), Cu (II), Zn (II), Ni (II),	–	–	Adsorbent dosage: 0.002-0.016 g/100 mL; Metal ion concentration: 60ppm; pH: 3–9; contact time: 10–65 min; Temperature: 25–55 °C	Pb (II): 89.612 (pH 5) Cr (III): 92.033 (pH 6) Cu (II): 92.433 (pH 6) Zn (II): 90.383 (pH 7) Ni (II): 92.233 (pH 8)	Pb (II): 200.00 Cr (III): 24.330 Cu (II): 62.890 Zn (II): 63.690 Ni (II): 51.020	–	[142]
Functionalized lignin-based magnetic adsorbents (L1@MNP)	Covalent cross-linking	Pb (II)	23.33	–	Adsorbent dosage: 10 g/25mL; Metal ion concentration: 200 ppm; pH: 2–6; contact time: 5–240 min; temperature: 25 °C	~88 (pH 5)	111.23 (pH 5)	5	[143]
Fe_3O_4-ZnO/RBC-DES	Multi-steps coating and deep eutectic solvent doping	Cr (VI), Pb (II), diclofenac sodium (DCF)	57.96	0.161	Adsorbent dosage: 2 g/L; Initial Cr (VI) and Pb (II) concentration: 50 mg/L, DCF 20 mg/L; Volume: 25mL; pH 2 for Cr (VI), DCF and pH 6 for Pb (II)	Cr (VI): 95.1 Pb (II): ~100 DCF: 69.2	Cr (VI): 66.23 Pb (II): 384.62 DCF: 24.33	5	[144]
Magnetic graphene oxide (MGO)	Co-precipitation	*Escherichia coli* (*E. coli*), *Yersina ruckeri* (*Y. ruckeri*), *Antobacter agglomerans* (*A. agglomerans*)	–	–	Adsorbent dosage: 0.1–0.6 g mg/mL; incubation temperature: 37 °C; incubation time: 18 h	*E. coli*: 98.787 (0.5 mg/mL) *Y. ruckeri*: 97.150 (0.5 mg/mL) *A. agglomerans*: 97.689 (0.45mg/mL)	–	–	[142]

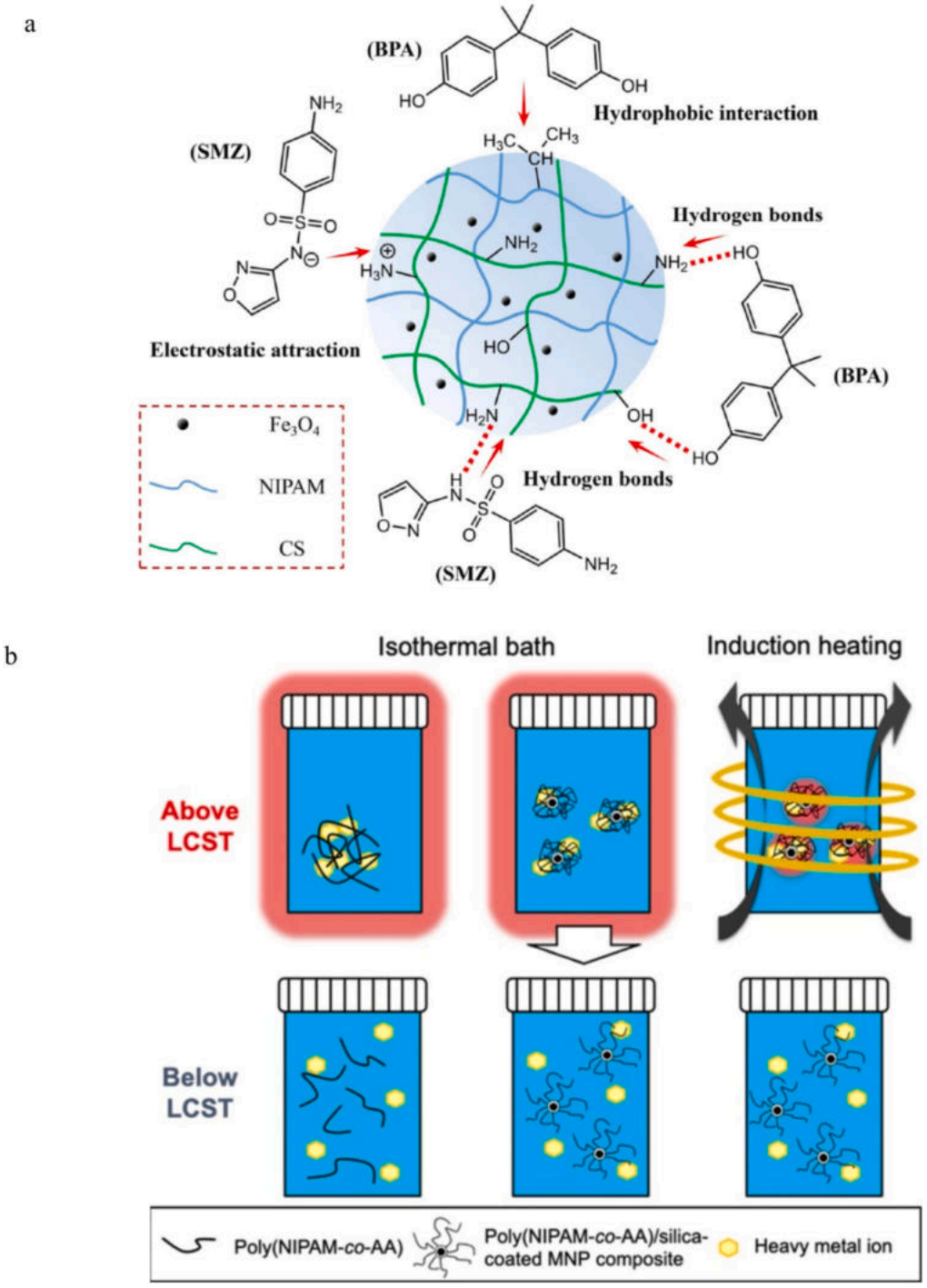

Fig. 7. (a) Adsorption mechanism of SMZ and BPA by the magnetic hydrogel [146]. (b) Schematic diagram shows the adsorption mechanisms for heavy metal ions by poly(NIPAM-*co*-AA)/silica-coated MNP composite [148]. Reproduced with permission from [146,148].

the ability to degrade the antibiotics mentioned and antibacterial effect, whereas the superparamagnetic property of Fe_3O_4 provides recyclability towards the synthesized nanocomposite by applying an external magnetic field.

Yee and colleagues [154] developed the pH-magnetic-light trifunctionalities microspheres through the incorporation of POMs as potential photocatalyst into poly(diallyldimethylammonium chloride) (PDDA) functionalized Fe_3O_4 nanoparticles within polyethersulfone (PES) matrix for the removal of methylene blue (MB) and methyl orange (MO) dyes. POMs play the role in effectively degrading the dye molecules through photocatalysis, also pH sensitivity of POMs provides the composite ability to adsorb both cationic MB and anionic MO by varying the pH of the medium, and rapid separation owing to the magnetism property.

3. Discussion and future prospective

Smart materials represent the future generation and drive the transformation of water treatment methodologies. However, the study of smart materials in water treatment is still nascent, especially the development and application of multi-stimuli responsive smart materials, with the scientific community just beginning to scratch the surface

Table 3
Summary of reported magnetic and thermal responsive smart materials for water treatment application.

Magnetic and thermal responsive compounds	Fabrication method	Pollutants	Surface area (m^2/g)	Pore volume (cm^3/g)	Operational conditions	Removal efficiency (%)	Adsorption capacity (mg/g)	Reusability (cycle)	References
Magnetic poly(N-isopropylacrylamide)/chitosan hydrogel	Interpenetrating network (IPN)	Sulfamethoxazole (SMZ), bisphenol A (BPA)	60.70	0.0672	Adsorbent dosage: 0.25-3.5 g/20 mL; ECs concentration: 10 μg/L; mixing speed: 250 rpm; temperature: 25–45 °C	–	SMZ: 33.95 BPA: 467.11	5	[146]
Fe@p(NIPAM-co-DMMA)	Free radical in-situ polymerization	Sudan red dye	–	–	Adsorbent dosage: 50 mg/100 mL; Dye concentration: 10 μg/L; contact time: 50 min; temperature: 35 °C	~96	–	–	[147]
Fe@SiO_2@PNIPAM-co-MAA	Free radical in-situ polymerization	Bisphenol A, phenol, hydroquinone	–	–	Adsorbent dosage: 40 mg/100 mL; phenols concentration: 10 μg/L; contact time: 40 min; temperature: 25–45 °C	Bisphenol A: ~87 Phenol: ~80 Hydroquinone: ~90	–	–	[151]
(PNIPAM-co-AA)-silica-PVP-MNPs	Free radical in-situ polymerization	Cr (III)	–	–	Adsorbent dosage: 4 mg/100 mL; Cr (III) concentration: 20–100 ppm; pH: 5; contact time: 24 h; mixing speed: 40 rpm temperature: 25–45 °C	28.34 (25 °C)	243.90	–	[149]
Poly(NIPAM-co-AA)/silica-coated MNP composite	Electro-oxidation	Cu (II)	–	–	Adsorbent dosage: 50 mg/10 mL; Cu (III) concentration: 0.25–2.5 mM; pH: 5; contact time: 4 h; temperature: 10 °C and 60 °C	–	0.511 mmol/g	5	[148]
Fe_3O_4@poly(NIPAm-*co*-AGE)@DFFPBA	Surface-initiated atom transfer radical polymerization	*Salmonella* spp., *S. aureus*	–	–	Adsorbent dosage: 2 mg/1 mL; Bacterial suspension: OD_{600} ~ 1.4; pH: 6.5 to 8.0; mixing speed: 150 rpm; contact time: 15 min; temperature: 20 °C and 40 °C	–	*Salmonella* spp.: 50.98×10^6 cfu/mg *S. aureus*: 32.14 $\times 10^6$ cfu/mg	4	[150]

of its potential. Most adsorption or degradation experiments using smart materials are conducted to remove the organic dyes, and very few research articles are available to remove inorganic heavy metal ions, inorganic non-metallic, and microbial pollutants. Real wastewater significantly differs from artificially synthesized water samples, particularly due to the diverse array of pollutants present. Unlike synthetic samples, which may contain a limited selection of pollutants in controlled concentrations, real wastewater represents a complex mixture of organic, inorganic, and microbial contaminants originating from various industrial, agricultural, and domestic sources. Therefore, more research should be conducted to evaluate the removal efficiency of toxic heavy metal ions, non-metallic ions, and microbial pollutants, in conjunction with using real wastewater to study and establish the smart materials, ensuring the practicality and commercialization of the smart materials.

Furthermore, the low reusability of current adsorbents or photocatalysts in water treatment poses a significant challenge. Such a downfall is mainly attributable to pore blockage caused by incomplete desorption, deterioration of the adsorbent structure and reduction in the specific surface area of the adsorbents after several cycles of reuse. The conventional technique used to regenerate adsorbents is toxic eluent. However, the excessive usage of eluent may destroy the adsorbent structure and poses secondary pollution during eluent disposal. In light of these challenges, developing self-cleaning adsorbents or photocatalysts has emerged as a promising solution. These innovative materials possess the ability to regenerate or clean themselves, thereby extending their lifespan and enhancing their reusability. Harnessing mechanisms such as photocatalysis (light-responsive smart materials) and phase transition (thermal-responsive materials) can effectively mitigate fouling and maintain pollutant removal efficacy over multiple cycles.

In addition, the development of multi-stimuli responsive smart materials is still in its early stages. Despite the demonstrated effectiveness of multi-stimuli responsive materials in water treatment, research in this area is still very limited, with only preliminary studies conducted thus far. The limited scope of research hinders our understanding of the material's full range of capabilities and potential applications. Therefore, it is imperative to conduct more comprehensive and meticulous studies to explore their fundamental, performance, mechanisms, and practical implications in water treatment application.

Current trends in the dynamic water treatment field highlight significant advancements in product development instead of process development. Product development focuses on creating innovative materials (advanced stimuli-responsive materials) and technologies (filtration systems, membrane technologies and disinfection methods), contributing significantly to the efficacy of water treatment systems and ensuring higher water quality standards, which overall is crucial for advancing water treatment technologies. However, there is an overemphasis on product development and without concurrent process development, these technological innovations may not reach their full potential. Process development focuses on refining operational strategies, optimizing system parameters, reducing waste generation and ensuring system robustness and scalability. A balanced approach between product and process development ensures that the novel products are technically superior, practical, and economically viable. Therefore, achieving a balanced approach is essential to maximize the effectiveness and impact of innovations in the water treatment field.

Smart materials possess unique properties that enable them to respond dynamically to environmental changes, offering promising solutions to the challenges faced in water treatment processes. There is a growing recognition of the need for further investigation and development to harness the capabilities of smart materials for water treatment fully. As researchers delve deeper into this field, innovative applications and more efficient water treatment solutions are anticipated to emerge, ultimately paving the way for a more sustainable and practical approach to water treatment.

4. Conclusion

Research into smart materials' development and diverse applications have gained momentum in recent years. This review summarizes the synthesis and applications of various categories of stimuli-responsive smart materials to remove diverse contaminants including organic, inorganic and microbial pollutants. Stimuli-responsive materials in water treatment offer a sophisticated approach by exhibiting tuneable properties that respond to internal or external stimuli. This capability allows for enhanced controllability over pollutant removal from water. These smart materials can selectively adsorb or release contaminants based on specific triggers/stimuli such as temperature, light, magnetic or pH, optimizing resource utilization and improving water treatment efficiency. The single-stimulus responsive smart materials reported in this review have demonstrated exciting and convincing performance for the uptake of different nature types of pollutants under varying conditions. Despite the substantial potential for performance enhancement offered by single-stimulus responsive materials, limiting challenges such as recoverability and reusability need to be addressed. Combining several stimuli-responsive materials in a single entity provides a versatile and practical approach to tackle the challenges associated with recoverability and reusability. For instance, the incorporation of magnetic nanoparticles in forming a composite offers the benefit of facile and rapid separation, while the introduction of thermal-responsive materials such as PNIPAM demonstrates the uptake and release of pollutants in response to temperature changes which emphasizes the importance of self-cleaning property in terms of sustainability and reusability to be exerted by modern era smart materials for water treatment application. However, research in developing and applying multi-stimuli responsive smart materials remains limited, with only preliminary studies conducted so far. Hence more work is needed in this vein. Moreover, the practicality of these smart materials in treating real wastewater comprising diverse pollutants cannot be overlooked to realize their real-life applicability and commercial viability in water treatment applications. A vast scope of research and development activities lies ahead for forging a path towards a more sustainable and practical approach in the water treatment field.

CRediT authorship contribution statement

Soon Wah Goh: Writing – review & editing, Writing – original draft, Validation, Conceptualization. **Qi Hwa Ng:** Writing – review & editing, Visualization, Validation, Supervision, Conceptualization. **Siti Kartini Enche Ab Rahim:** Validation, Supervision. **Siew Chun Low:** Writing – review & editing, Validation, Supervision. **Peng Yong Hoo:** Writing – review & editing, Validation. **Ryan Yow Zhong Yeo:** Writing – review & editing, Validation. **Thiam Leng Chew:** Writing – review & editing, Validation. **Zeinab Abbas Jawad:** Writing – review & editing, Validation.

Declaration of competing interest

The authors declare that they have no known competing financial interests or personal relationships that could have appeared to influence the work reported in this paper.

Acknowledgements

The authors would like to acknowledge the support from the Fundamental Research Grant Scheme (FRGS) under grant number of FRGS/1/2021/TK0/UNIMAP/02/3 from the Ministry of Higher Education Malaysia. Furthermore, sincere indebtedness and gratitude are addressed to Universiti Malaysia Perlis (UniMAP).

Appendix A. Supplementary data

Supplementary data to this article can be found online at https://doi.org/10.1016/j.jwpe.2025.106993.

Data availability

The authors do not have permission to share data.

References

[1] J. Zhao, Y. Wang, X. Zhang, Q. Liu, Industrial and agricultural water use efficiency and influencing factors in the process of urbanization in the middle and lower reaches of the Yellow River Basin, China, Land 11 (8) (Aug. 2022) 1248, https://doi.org/10.3390/LAND11081248, 2022, Vol. 11, Page 1248.
[2] F. Lu, D. Astruc, Nanocatalysts and other nanomaterials for water remediation from organic pollutants, Coord. Chem. Rev. 408 (Apr. 2020) 213180, https://doi.org/10.1016/J.CCR.2020.213180.
[3] J. Wang, Z. Wang, C.L.Z. Vieira, J.M. Wolfson, G. Pingtian, S. Huang, Review on the treatment of organic pollutants in water by ultrasonic technology, Ultrason. Sonochem. 55 (Jul. 2019) 273–278, https://doi.org/10.1016/J.ULTSONCH.2019.01.017.
[4] P. Singh, et al., Systematic review on applicability of magnetic iron oxides–integrated photocatalysts for degradation of organic pollutants in water, Mater Today Chem 14 (Dec. 2019) 100186, https://doi.org/10.1016/J.MTCHEM.2019.08.005.
[5] X. Zhang, et al., Urban drought challenge to 2030 sustainable development goals, Sci. Total Environ. 693 (Nov. 2019) 133536, https://doi.org/10.1016/J.SCITOTENV.2019.07.342.
[6] M. Irannezhad, B. Ahmadi, J. Liu, D. Chen, J.H. Matthews, Global water security: a shining star in the dark sky of achieving the sustainable development goals, Sustainable Horizons 1 (Jan. 2022) 100005, https://doi.org/10.1016/J.HORIZ.2021.100005.
[7] J.D. Sachs, G. Schmidt-Traub, M. Mazzucato, D. Messner, N. Nakicenovic, J. Rockström, Six transformations to achieve the sustainable development goals, Nature Sustainability 2019 2:9 2 (9) (Aug. 2019) 805–814, https://doi.org/10.1038/s41893-019-0352-9.
[8] G. Crini, E. Lichtfouse, L.D. Wilson, N. Morin-Crini, Conventional and non-conventional adsorbents for wastewater treatment, Environ. Chem. Lett. 17 (1) (Mar. 2019) 195–213, https://doi.org/10.1007/S10311-018-0786-8/METRICS.
[9] P. Samanta, A.V. Desai, S. Let, S.K. Ghosh, Advanced porous materials for sensing, capture and detoxification of organic pollutants toward water remediation, ACS Sustain. Chem. Eng. 7 (8) (Apr. 2019) 7456–7478, https://doi.org/10.1021/ACSSUSCHEMENG.9B00155/ASSET/IMAGES/MEDIUM/SC-2019-00155Q_0022.GIF.
[10] M.I.A. Abdel Maksoud, A.M. Elgarahy, C. Farrell, A.H. Al-Muhtaseb, D. W. Rooney, A.I. Osman, Insight on water remediation application using magnetic nanomaterials and biosorbents, Coord. Chem. Rev. 403 (Jan. 2020) 213096, https://doi.org/10.1016/J.CCR.2019.213096.
[11] T.A. Saleh, M. Mustaqeem, M. Khaled, Water treatment technologies in removing heavy metal ions from wastewater: a review, Environ Nanotechnol Monit Manag 17 (May 2022) 100617, https://doi.org/10.1016/J.ENMM.2021.100617.
[12] H. Abu Hasan, M.H. Muhammad, N.I. Ismail, A review of biological drinking water treatment technologies for contaminants removal from polluted water resources, Journal of Water Process Engineering 33 (Feb. 2020) 101035, https://doi.org/10.1016/J.JWPE.2019.101035.
[13] T.X. Zhang, M.R. Li, C. Liu, S.P. Wang, Z.G. Yan, A review of the toxic effects of ammonia on invertebrates in aquatic environments, Environ. Pollut. 336 (Nov. 2023) 122374, https://doi.org/10.1016/J.ENVPOL.2023.122374.
[14] C. Shi, X. Wang, S. Zhou, X. Zuo, C. Wang, Mechanism, application, influencing factors and environmental benefit assessment of steel slag in removing pollutants from water: a review, Journal of Water Process Engineering 47 (Jun. 2022) 102666, https://doi.org/10.1016/J.JWPE.2022.102666.
[15] X. Wen, et al., Microbial indicators and their use for monitoring drinking water quality—a review, Sustainability 12 (6) (Mar. 2020) 2249, https://doi.org/10.3390/SU12062249, 2020, Vol. 12, Page 2249.
[16] K.M. Hamdi, S. Lihan, N. Hamdan, T.M. Guan, Water quality assessment and the prevalence of antibioticresistant bacteria from a recreational river in Kuching, Sarawak, Malaysia, J. Sustain. Sci. Manag. 17 (5) (May 2022) 2672–7226, https://doi.org/10.46754/JSSM.2022.05.004.
[17] N. Saeidi, et al., Occurrence of traditional and alternative fecal indicators in tropical urban environments under different land use patterns, Appl. Environ. Microbiol. 84 (14) (Jul. 2018), https://doi.org/10.1128/AEM.00287-18/SUPPL_FILE/ZAM014188631S1.PDF.
[18] H. Mittal, V. Kumar, Saruchi, S.S. Ray, Adsorption of methyl violet from aqueous solution using gum xanthan/Fe3O4 based nanocomposite hydrogel, Int. J. Biol. Macromol. 89 (Aug. 2016) 1–11, https://doi.org/10.1016/J.IJBIOMAC.2016.04.050.
[19] M.D. Faysal Hossain, N. Akther, Y. Zhou, Recent advancements in graphene adsorbents for wastewater treatment: current status and challenges, Chin. Chem. Lett. 31 (10) (Oct. 2020) 2525–2538, https://doi.org/10.1016/J.CCLET.2020.05.011.

[20] F. Younas, et al., Current and emerging adsorbent technologies for wastewater treatment: trends, limitations, and environmental implications, Water 13 (2) (Jan. 2021) 215, https://doi.org/10.3390/W13020215, 2021, Vol. 13, Page 215.
[21] V. Gadore, M. Ahmaruzzaman, Smart materials for remediation of aqueous environmental contaminants, J. Environ. Chem. Eng. 9 (6) (Dec. 2021) 106486, https://doi.org/10.1016/J.JECE.2021.106486.
[22] T. Ramakrishnan, et al., Recent developments in stimuli responsive smart materials and applications: An overview, J. Nanomater. 2022 (1) (Jan. 2022) 4031059, https://doi.org/10.1155/2022/4031059.
[23] Y. Stetsyshyn, et al., Temperature-responsive and multi-responsive grafted polymer brushes with transitions based on critical solution temperature: synthesis, properties, and applications, Colloid and Polymer Science 299 (3) (Sep. 2020) 363–383, https://doi.org/10.1007/S00396-020-04750-0, 2020 299:3.
[24] A. Halperin, M. Kröger, F.M. Winnik, Poly(N-isopropylacrylamide) phase diagrams: fifty years of research, Angew. Chem. Int. Ed. 54 (51) (Dec. 2015) 15342–15367, https://doi.org/10.1002/ANIE.201506663.
[25] L. Tang, L. Wang, X. Yang, Y. Feng, Y. Li, W. Feng, Poly(N-isopropylacrylamide)-based smart hydrogels: design, properties and applications, Prog. Mater. Sci. 115 (Jan. 2021) 100702, https://doi.org/10.1016/J.PMATSCI.2020.100702.
[26] K. Yanase, R. Buchner, T. Sato, Microscopic insights into the phase transition of poly(N-isopropylacrylamide) in aqueous media: effects of molecular weight and polymer concentration, J. Mol. Liq. 302 (Mar. 2020) 112025, https://doi.org/10.1016/J.MOLLIQ.2019.112025.
[27] Y. Kotsuchibashi, Recent advances in multi-temperature-responsive polymeric materials, Polymer Journal 52 (7) (Mar. 2020) 681–689, https://doi.org/10.1038/s41428-020-0330-0, 2020 52:7.
[28] M. Cao, et al., Extraction-like removal of organic dyes from polluted water by the graphene oxide/PNIPAM composite system, Chem. Eng. J. 405 (Feb. 2021) 126647, https://doi.org/10.1016/J.CEJ.2020.126647.
[29] Y. Guo, X. Zhang, X. Sun, D. Kong, M. Han, X. Wang, Nanoadsorbents based on NIPAM and citric acid: removal efficacy of heavy metal ions in different media, ACS Omega 4 (10) (Sep. 2019) 14162–14168, https://doi.org/10.1021/ACSOMEGA.9B00573/ASSET/IMAGES/MEDIUM/AO9B00573_M002.GIF.
[30] E.M. Frazar, R.A. Shah, T.D. Dziubla, J.Z. Hilt, Multifunctional temperature-responsive polymers as advanced biomaterials and beyond, J. Appl. Polym. Sci. 137 (25) (Jul. 2020) 48770, https://doi.org/10.1002/APP.48770.
[31] W.J. Lim, B.S. Ooi, Applications of responsive hydrogel to enhance the water recovery via membrane distillation and forward osmosis: a review, Journal of Water Process Engineering 47 (Jun. 2022) 102828, https://doi.org/10.1016/J.JWPE.2022.102828.
[32] J. Yang, K. Wang, Z. Lv, W. Li, K. Luo, Z. Cao, Facile preparation and dye adsorption performance of poly(N-isopropylacrylamide-co-acrylic acid)/molybdenum disulfide composite hydrogels, ACS Omega 6 (42) (Oct. 2021) 28285–28296, https://doi.org/10.1021/ACSOMEGA.1C04433/ASSET/IMAGES/MEDIUM/AO1C04433_M008.GIF.
[33] B. Pany, et al., Polymerized stimuli-responsive microgels for the removal of organic dye from water, J. Mol. Liq. 375 (Apr. 2023) 121267, https://doi.org/10.1016/J.MOLLIQ.2023.121267.
[34] K. Murakami, A. Imai, A. Nakamura, Temperature dependence of aggregation behavior and dye adsorption of poly(N-isopropylacrylamide) hydrogel/mesoporous silica composites, Colloids Surf. A Physicochem. Eng. Asp. 674 (Oct. 2023) 131944, https://doi.org/10.1016/J.COLSURFA.2023.131944.
[35] S.P. Sridhar, J. John, R. Kumar, R. Shunmugam, C. Saravanan, B. Joseph, Chemically crosslinked poly(N-isopropylacrylamide-block-4-vinylpyridine) organogel with myriad applications, Mater. Lett. 272 (Aug. 2020) 127854, https://doi.org/10.1016/J.MATLET.2020.127854.
[36] Q. Wang, Y. Xiong, J. Xu, F. Dong, Y. Xiong, Oxidation-resistant cyclodextrin-encapsulated-MXene/poly (N-isopropylacrylamide) composite hydrogel as a thermosensitive adsorbent for phenols, Sep. Purif. Technol. 286 (Apr. 2022) 120506, https://doi.org/10.1016/J.SEPPUR.2022.120506.
[37] H. Tokuyama, M. Hamazaki, M. Kubota, Temperature-swing adsorption of 4-isopropylphenol and bisphenol A onto a poly(N-isopropylacrylamide)/silica gel composite, Mater Today Commun 33 (Dec. 2022) 104755, https://doi.org/10.1016/J.MTCOMM.2022.104755.
[38] M. Kafetzi, K.B.L. Borchert, C. Steinbach, D. Schwarz, S. Pispas, S. Schwarz, Thermoresponsive PNIPAM-b-PAA block copolymers as 'smart' adsorbents of Cu (II) for water restore treatments, Colloids Surf. A Physicochem. Eng. Asp. 614 (Apr. 2021) 126049, https://doi.org/10.1016/J.COLSURFA.2020.126049.
[39] H. Luo, et al., Phosphorus removal and recovery from water with macroporous bead adsorbent constituted of alginate-Zr4+ and PNIPAM-interpenetrated networks, Int. J. Biol. Macromol. 126 (Apr. 2019) 1133–1144, https://doi.org/10.1016/J.IJBIOMAC.2018.12.269.
[40] T. Chen, et al., Smart copolymer surface derived from geminized cationic amphiphilic polymers for reversibly switchable bactericidal and self-cleaning abilities, Langmuir 39 (30) (Aug. 2023) 10521–10529, https://doi.org/10.1021/ACS.LANGMUIR.3C01005/SUPPL_FILE/LA3C01005_SI_001.PDF.
[41] B. Wang, et al., Copolymer brushes with temperature-triggered, reversibly switchable bactericidal and antifouling properties for biomaterial surfaces, ACS Appl. Mater. Interfaces 8 (40) (Oct. 2016) 27207–27217, https://doi.org/10.1021/ACSAMI.6B08893/ASSET/IMAGES/MEDIUM/AM-2016-088932_0013.GIF.
[42] R. Ameta, M.S. Solanki, S. Benjamin, S.C. Ameta, Photocatalysis, in: Advanced Oxidation Processes for Wastewater Treatment: Emerging Green Chemical Technology, Jan. 2018, pp. 135–175, https://doi.org/10.1016/B978-0-12-810499-6.00006-1.
[43] X. Lang, J. Zhao, X. Chen, Visible-light-induced photoredox catalysis of dye-sensitized titanium dioxide: selective aerobic oxidation of organic sulfides, Angew. Chem. 128 (15) (Apr. 2016) 4775–4778, https://doi.org/10.1002/ANGE.201600405.
[44] M.C. Wu, J.S. Chih, W.K. Huang, Bismuth doping effect on TiO2 nanofibres for morphological change and photocatalytic performance, CrystEngComm 16 (46) (Nov. 2014) 10692–10699, https://doi.org/10.1039/C4CE01348D.
[45] N. Sedaghati, A. Habibi-Yangjeh, M. Pirhashemi, S. Vadivel, Boosted visible-light photocatalytic performance of TiO2-x decorated by BiOI and AgBr nanoparticles, J Photochem Photobiol A Chem 384 (Nov. 2019) 112066, https://doi.org/10.1016/J.JPHOTOCHEM.2019.112066.
[46] S. Pandey, K.K. Mandari, J. Kim, M. Kang, E. Fosso-Kankeu, Recent advancement in visible-light-responsive photocatalysts in heterogeneous photocatalytic water treatment technology, Photocatalysts in Advanced Oxidation Processes for Wastewater Treatment (May 2020) 167–196, https://doi.org/10.1002/9781119631422.CH6.
[47] E. Abkar, M. Ghanbari, O. Amiri, M. Salavati-Niasari, Facile preparation and characterization of a novel visible-light-responsive Rb 2 HgI 4 nanostructure photocatalyst, RSC Adv. 11 (49) (Sep. 2021) 30849–30859, https://doi.org/10.1039/D1RA03152J.
[48] H. Dong, et al., An overview on limitations of TiO2-based particles for photocatalytic degradation of organic pollutants and the corresponding countermeasures, Water Res. 79 (Aug. 2015) 128–146, https://doi.org/10.1016/J.WATRES.2015.04.038.
[49] H. Huang, et al., One-step in-situ preparation of N-doped TiO2@C derived from Ti3C2 MXene for enhanced visible-light driven photodegradation, Appl Catal B 251 (Aug. 2019) 154–161, https://doi.org/10.1016/J.APCATB.2019.03.066.
[50] I. Gul, et al., Solar light responsive bismuth doped titania with Ti3+ for efficient photocatalytic degradation of flumequine: synergistic role of peroxymonosulfate, Chem. Eng. J. 384 (Mar. 2020) 123255, https://doi.org/10.1016/J.CEJ.2019.123255.
[51] M. Norouzi, A. Fazeli, O. Tavakoli, Phenol contaminated water treatment by photocatalytic degradation on electrospun Ag/TiO2 nanofibers: optimization by the response surface method, Journal of Water Process Engineering 37 (Oct. 2020) 101489, https://doi.org/10.1016/J.JWPE.2020.101489.
[52] N.M. Ngoepe, M.M. Mathipa, N.C. Hintsho-Mbita, Biosynthesis of titanium dioxide nanoparticles for the photodegradation of dyes and removal of bacteria, Optik (Stuttg) 224 (Dec. 2020) 165728, https://doi.org/10.1016/J.IJLEO.2020.165728.
[53] X. Gao, P.G. Ren, J. Wang, F. Ren, Z. Dai, Y.L. Jin, Fabrication of visible-light responsive TiO2@C photocatalyst with an ultra-thin carbon layer to efficiently degrade organic pollutants, Appl. Surf. Sci. 532 (Dec. 2020) 147482, https://doi.org/10.1016/J.APSUSC.2020.147482.
[54] N. Raza, et al., Solar-light-active silver phosphate/titanium dioxide/silica heterostructures for photocatalytic removal of organic dye, J. Clean. Prod. 254 (May 2020) 120031, https://doi.org/10.1016/J.JCLEPRO.2020.120031.
[55] X. Lu, et al., Titanium dioxide coated carbon foam as microreactor for improved sunlight driven treatment of cotton dyeing wastewater, J. Clean. Prod. 246 (Feb. 2020) 118949, https://doi.org/10.1016/J.JCLEPRO.2019.118949.
[56] Y. Chen, A. Li, X. Fu, Z. Peng, Electrospinning-based (N,F)-co-doped TiO2-δ nanofibers: an excellent photocatalyst for degrading organic dyes and heavy metal ions under visible light, Mater. Chem. Phys. 291 (Nov. 2022) 126672, https://doi.org/10.1016/J.MATCHEMPHYS.2022.126672.
[57] J. Musial, D.T. Mlynarczyk, B.J. Stanisz, Photocatalytic degradation of sulfamethoxazole using TiO2-based materials – perspectives for the development of a sustainable water treatment technology, Sci. Total Environ. 856 (Jan. 2023) 159122, https://doi.org/10.1016/J.SCITOTENV.2022.159122.
[58] K.P. Gopinath, N.V. Madhav, A. Krishnan, R. Malolan, G. Rangarajan, Present applications of titanium dioxide for the photocatalytic removal of pollutants from water: a review, J. Environ. Manage. 270 (Sep. 2020) 110906, https://doi.org/10.1016/J.JENVMAN.2020.110906.
[59] M. Moradi, A. Naderi, N. Bahari, M. Harati, J. Rodríguez-Chueca, R. Rezaei Kalantary, Visible-light-driven photocatalytic inactivation of Escherichia coli by titanium dioxide anchored on natural pyrite, Inorg. Chem. Commun. 144 (Oct. 2022) 109913, https://doi.org/10.1016/J.INOCHE.2022.109913.
[60] K. Suzuki, N. Mizuno, K. Yamaguchi, Polyoxometalate photocatalysis for liquid-phase selective organic functional group transformations, ACS Catal. 8 (11) (Nov. 2018) 10809–10825, https://doi.org/10.1021/ACSCATAL.8B03498/ASSET/IMAGES/MEDIUM/CS-2018-034989_0032.GIF.
[61] B. D'Cruz, J. Samuel, M.K. Sreedhar, L. George, Green synthesis of novel polyoxoanions of tungsten containing phosphorus as a heteroatom: characterization, non-isothermal decomposition kinetics and photocatalytic activity, New J. Chem. 38 (11) (Oct. 2014) 5436–5444, https://doi.org/10.1039/C4NJ01098A.
[62] N. Fang, et al., Synthesis and adsorption properties of [Cu(L) 2 (H 2 O)]H 2 [Cu(L) 2 (P 2 Mo 5 O 23)]·4H 2 O/Fe 3 O 4 nanocomposites, RSC Adv. 7 (41) (May 2017) 25325–25333, https://doi.org/10.1039/C7RA02133J.
[63] Y. Guo Zheng, W. Xue, A new 3D POMOF built upon Keggin clusters and flexible n-heterocycle carboxylate ligands for catalytic and antimicrobial properties, Inorg Chem Commun 141 (Jul. 2022) 109520, https://doi.org/10.1016/J.INOCHE.2022.109520.
[64] H. Shi, et al., Pt/POMs/TiO2 composite nanofibers with an enhanced visible-light photocatalytic performance for environmental remediation, Dalton Trans. 48 (35) (Sep. 2019) 13353–13359, https://doi.org/10.1039/C9DT02965F.

[65] J.J. Walsh, A.M. Bond, R.J. Forster, T.E. Keyes, Hybrid polyoxometalate materials for photo(electro-) chemical applications, Coord. Chem. Rev. 306 (P1) (Jan. 2016) 217–234, https://doi.org/10.1016/J.CCR.2015.06.016.

[66] S.Y. Lai, K.H. Ng, C.K. Cheng, H. Nur, M. Nurhadi, M. Arumugam, Photocatalytic remediation of organic waste over Keggin-based polyoxometalate materials: a review, Chemosphere 263 (Jan. 2021) 128244, https://doi.org/10.1016/J.CHEMOSPHERE.2020.128244.

[67] M. Mon, R. Bruno, J. Ferrando-Soria, D. Armentano, E. Pardo, Metal–organic framework technologies for water remediation: towards a sustainable ecosystem, J Mater Chem A Mater 6 (12) (Mar. 2018) 4912–4947, https://doi.org/10.1039/C8TA00264A.

[68] X. Zhao, et al., Polyoxometalate-based metal-organic frameworks as visible-light-induced photocatalysts, Inorg. Chem. 57 (9) (May 2018) 5030–5037, https://doi.org/10.1021/ACS.INORGCHEM.8B00098/SUPPL_FILE/IC8B00098_SI_001.PDF.

[69] L. Hou, et al., Reduced phosphomolybdate hybrids as efficient visible-light photocatalysts for Cr(VI) reduction, Inorg. Chem. 58 (24) (Dec. 2019) 16667–16675, https://doi.org/10.1021/ACS.INORGCHEM.9B02777/SUPPL_FILE/IC9B02777_SI_001.PDF.

[70] L. Wang, et al., Synthesis of polyoxometalates (POM)/TiO2/Cu and removal of nitrate nitrogen in water by photocatalysis, Chemosphere 278 (Sep. 2021) 130298, https://doi.org/10.1016/J.CHEMOSPHERE.2021.130298.

[71] X. An, Q. Tang, H. Lan, H. Liu, J. Qu, Polyoxometalates/TiO2 Fenton-like photocatalysts with rearranged oxygen vacancies for enhanced synergetic degradation, Appl Catal B 244 (May 2019) 407–413, https://doi.org/10.1016/J.APCATB.2018.11.063.

[72] Q. Tang, X. An, H. Lan, H. Liu, J. Qu, Polyoxometalates/TiO2 photocatalysts with engineered facets for enhanced degradation of bisphenol A through persulfate activation, Appl Catal B 268 (Jul. 2020) 118394, https://doi.org/10.1016/J.APCATB.2019.118394.

[73] H. Shi, et al., Polyoxometalate/TiO2/Ag composite nanofibers with enhanced photocatalytic performance under visible light, Appl Catal B 221 (Feb. 2018) 280–289, https://doi.org/10.1016/J.APCATB.2017.09.027.

[74] F. Lin, Y. Yang, Z. Zhang, N. Tang, G. Zhu, A titania-supported polyoxometalate and au cocatalyst for efficient photocatalytic environmental remediation, Catalysts 11 (9) (Sep. 2021) 1045, https://doi.org/10.3390/CATAL11091045/S1.

[75] J. Guan, et al., Enhanced solar-photocatalytic activity for the simultaneous degradation and detoxification of multiple chlorophenols by embedding plasmonic Pt into TiO2/H3PW12O40 nanopore, Appl. Surf. Sci. 513 (May 2020) 145833, https://doi.org/10.1016/J.APSUSC.2020.145833.

[76] X. Tian, Y. Zhang, Y. Ma, Q. Zhao, Z. Han, Hourglass-type polyoxometalate-based crystalline materials as efficient cooperating photocatalysts for the reduction of Cr(VI) and oxidation of dyes, Cat. Sci. Technol. 10 (8) (Apr. 2020) 2593–2601, https://doi.org/10.1039/D0CY00208A.

[77] M.A. Lafta, S.H. Ammar, H.J. Khadim, Z.H. Jabbar, Improved photocatalytic degradation of methyl violet dye and pathogenic bacteria using g-C3N4 supported phosphotungstic acid heterojunction, J Photochem Photobiol A Chem 437 (Mar. 2023) 114506, https://doi.org/10.1016/J.JPHOTOCHEM.2022.114506.

[78] S.H. Ammar, H.J. Khadim, A. Isam Mohamed, Z.H. Jabbar, Synthesis of heterostructure composite (g-C3N4/phosphomolybdic acid) for synergistic piezo/photo-catalytic degradation of CR dye and S. aureus bacteria, J. Photochem. Photobiol. A Chem. 447 (Jan. 2024) 115243, https://doi.org/10.1016/J.JPHOTOCHEM.2023.115243.

[79] R. Pagano, S. Bettini, M. Ottolini, G. Ciccarella, L. Valli, G. Giancane, Piezo- and photo-responsive ZnO nanostructures for efficient tetracycline water remediation, Colloids Surf. A Physicochem. Eng. Asp. 680 (Jan. 2024) 132626, https://doi.org/10.1016/J.COLSURFA.2023.132626.

[80] I. Mahboob, et al., Effect of active species scavengers in photocatalytic desulfurization of hydrocracker diesel using mesoporous Ag3VO4, Chem. Eng. J. 441 (Aug. 2022) 136063, https://doi.org/10.1016/J.CEJ.2022.136063.

[81] K. Qiao, et al., Application of magnetic adsorbents based on iron oxide nanoparticles for oil spill remediation: a review, J. Taiwan Inst. Chem. Eng. 97 (Apr. 2019) 227–236, https://doi.org/10.1016/J.JTICE.2019.01.029.

[82] D.H.K. Reddy, Y.S. Yun, Spinel ferrite magnetic adsorbents: alternative future materials for water purification? Coord. Chem. Rev. 315 (May 2016) 90–111, https://doi.org/10.1016/J.CCR.2016.01.012.

[83] G. de V. Brião, J.R. de Andrade, M.G.C. da Silva, M.G.A. Vieira, Removal of toxic metals from water using chitosan-based magnetic adsorbents. a review, Environmental Chemistry Letters 18 (4) (Apr. 2020) 1145–1168, https://doi.org/10.1007/S10311-020-01003-Y, 2020 18:4.

[84] A.M. Gutierrez, T.D. Dziubla, J.Z. Hilt, Recent advances on iron oxide magnetic nanoparticles as sorbents of organic pollutants in water and wastewater treatment, Rev. Environ. Health 32 (1–2) (Mar. 2017) 111–117, https://doi.org/10.1515/REVEH-2016-0063/MACHINEREADABLECITATION/RIS.

[85] C. Martinez-Boubeta, K. Simeonidis, Magnetic nanoparticles for water purification, Nanoscale Materials in Water Purification (Jan. 2019) 521–552, https://doi.org/10.1016/B978-0-12-813926-4.00026-4.

[86] M. Mahdavi, et al., Synthesis, surface modification and characterisation of biocompatible magnetic Iron oxide nanoparticles for biomedical applications, Molecules 18 (7) (Jun. 2013) 7533–7548, https://doi.org/10.3390/MOLECULES18077533, 2013, Vol. 18, Pages 7533-7548.

[87] S. Ghosh, W. Jiang, J.D. McClements, B. Xing, Colloidal stability of magnetic iron oxide nanoparticles: influence of natural organic matter and synthetic polyelectrolytes, Langmuir 27 (13) (Jul. 2011) 8036–8043, https://doi.org/10.1021/LA200772E/ASSET/IMAGES/MEDIUM/LA-2011-00772E_0010.GIF.

[88] S.C.N. Tang, I.M.C. Lo, Magnetic nanoparticles: Essential factors for sustainable environmental applications, Water Res. 47 (8) (May 2013) 2613–2632, https://doi.org/10.1016/J.WATRES.2013.02.039.

[89] W.H. Chong, Q.H. Ng, J.K. Lim, S.P. Yeap, S.C. Low, Study on the enhancement of colloidal stable poly(sodium 4-styrene sulfonate) coated magnetite nanoparticles and regeneration capability for rapid magnetophoretic removal of organic dye, J. Chem. Technol. Biotechnol. 95 (12) (Dec. 2020) 3093–3104, https://doi.org/10.1002/JCTB.6485.

[90] C.S. Lee, et al., Synthesis of magnetic multi-walled carbon nanotubes via facile and solvent-free direct doping method for water remediation, Journal of Water Process Engineering 45 (Feb. 2022) 102487, https://doi.org/10.1016/J.JWPE.2021.102487.

[91] A. Bée, L. Obeid, R. Mbolantenaina, M. Welschbillig, D. Talbot, Magnetic chitosan/clay beads: a magsorbent for the removal of cationic dye from water, J. Magn. Magn. Mater. 421 (Jan. 2017) 59–64, https://doi.org/10.1016/J.JMMM.2016.07.022.

[92] H. Yang, et al., Rapid removal of anionic dye from water by poly(ionic liquid)-modified magnetic nanoparticles, J. Mol. Liq. 284 (Jun. 2019) 383–392, https://doi.org/10.1016/J.MOLLIQ.2019.04.029.

[93] Y. Long, L. Xiao, Q. Cao, Co-polymerization of catechol and polyethylenimine on magnetic nanoparticles for efficient selective removal of anionic dyes from water, Powder Technol. 310 (Apr. 2017) 24–34, https://doi.org/10.1016/J.POWTEC.2017.01.013.

[94] Y.R. Zhang, P. Su, J. Huang, Q.R. Wang, B.X. Zhao, A magnetic nanomaterial modified with poly-lysine for efficient removal of anionic dyes from water, Chem. Eng. J. 262 (Feb. 2015) 313–318, https://doi.org/10.1016/J.CEJ.2014.09.094.

[95] S. Pandey, A comprehensive review on recent developments in bentonite-based materials used as adsorbents for wastewater treatment, J. Mol. Liq. 241 (Sep. 2017) 1091–1113, https://doi.org/10.1016/J.MOLLIQ.2017.06.115.

[96] Y. Zhang, et al., Ultrafast adsorption of heavy metal ions onto functionalized lignin-based hybrid magnetic nanoparticles, Chem. Eng. J. 372 (Sep. 2019) 82–91, https://doi.org/10.1016/J.CEJ.2019.04.111.

[97] K. Chen, et al., Removal of cadmium and lead ions from water by sulfonated magnetic nanoparticle adsorbents, J. Colloid Interface Sci. 494 (May 2017) 307–316, https://doi.org/10.1016/J.JCIS.2017.01.082.

[98] I. Ali, et al., Encapsulated green magnetic nanoparticles for the removal of toxic Pb2+ and Cd2+ from water: development, characterization and application, J. Environ. Manage. 234 (Mar. 2019) 273–289, https://doi.org/10.1016/J.JENVMAN.2018.12.112.

[99] Q. Xu, W. Li, L. Ma, D. Cao, G. Owens, Z. Chen, Simultaneous removal of ammonia and phosphate using green synthesized iron oxide nanoparticles dispersed onto zeolite, Sci. Total Environ. 703 (Feb. 2020) 135002, https://doi.org/10.1016/J.SCITOTENV.2019.135002.

[100] S. Groiss, R. Selvaraj, T. Varadavenkatesan, R. Vinayagam, Structural characterization, antibacterial and catalytic effect of iron oxide nanoparticles synthesised using the leaf extract of Cynometra ramiflora, J. Mol. Struct. 1128 (Jan. 2017) 572–578, https://doi.org/10.1016/J.MOLSTRUC.2016.09.031.

[101] S. Vasantharaj, S. Sathiyavimal, P. Senthilkumar, F. LewisOscar, A. Pugazhendhi, Biosynthesis of iron oxide nanoparticles using leaf extract of Ruellia tuberosa: antimicrobial properties and their applications in photocatalytic degradation, J. Photochem. Photobiol. B 192 (Mar. 2019) 74–82, https://doi.org/10.1016/J.JPHOTOBIOL.2018.12.025.

[102] Y. Jin, J. Deng, J. Liang, C. Shan, M. Tong, Efficient bacteria capture and inactivation by cetyltrimethylammonium bromide modified magnetic nanoparticles, Colloids Surf. B Biointerfaces 136 (Dec. 2015) 659–665, https://doi.org/10.1016/J.COLSURFB.2015.10.009.

[103] M.S. Raghu, K. Yogesh Kumar, M.K. Prashanth, B.P. Prasanna, R. Vinuth, C. B. Pradeep Kumar, Adsorption and antimicrobial studies of chemically bonded magnetic graphene oxide-Fe3O4 nanocomposite for water purification, Journal of Water Process Engineering 17 (Jun. 2017) 22–31, https://doi.org/10.1016/J.JWPE.2017.03.001.

[104] J.K. Sahoo, S.K. Paikra, M. Mishra, H. Sahoo, Amine functionalized magnetic iron oxide nanoparticles: synthesis, antibacterial activity and rapid removal of Congo red dye, J. Mol. Liq. 282 (May 2019) 428–440, https://doi.org/10.1016/J.MOLLIQ.2019.03.033.

[105] G. Kocak, C. Tuncer, V. Bütün, pH-responsive polymers, Polym. Chem. 8 (1) (Dec. 2016) 144–176, https://doi.org/10.1039/C6PY01872F.

[106] F. Ofridam, M. Tarhini, N. Lebaz, É. Gagnière, D. Mangin, A. Elaissari, pH-sensitive polymers: classification and some fine potential applications, Polym. Adv. Technol. 32 (4) (Apr. 2021) 1455–1484, https://doi.org/10.1002/PAT.5230.

[107] H. Musarurwa, N. Tawanda Tavengwa, Recent progress in the application of pH-responsive polymers in separation science, Microchem. J. 179 (Aug. 2022) 107503, https://doi.org/10.1016/J.MICROC.2022.107503.

[108] S.R. Mane, A. Sathyan, R. Shunmugam, Biomedical applications of pH-responsive amphiphilic polymer nanoassemblies, ACS Appl Nano Mater 3 (3) (Mar. 2020) 2104–21117, https://doi.org/10.1021/ACSANM.0C00410/ASSET/IMAGES/MEDIUM/AN0C00410_0011.GIF.

[109] N. Deirram, C. Zhang, S.S. Kermaniyan, A.P.R. Johnston, G.K. Such, pH-responsive polymer nanoparticles for drug delivery, Macromol. Rapid Commun. 40 (10) (May 2019), https://doi.org/10.1002/MARC.201800917.

[110] M. Kanamala, W.R. Wilson, M. Yang, B.D. Palmer, Z. Wu, Mechanisms and biomaterials in pH-responsive tumour targeted drug delivery: a review, Biomaterials 85 (Apr. 2016) 152–167, https://doi.org/10.1016/J.BIOMATERIALS.2016.01.061.

[111] M. Rizwan, et al., pH sensitive hydrogels in drug delivery: brief history, properties, swelling, and release mechanism, material selection and applications, Polymers 9 (4) (Apr. 2017) 137, https://doi.org/10.3390/POLYM9040137, 2017, Vol. 9, Page 137.
[112] Y. Qin, L. Wang, C. Zhao, D. Chen, Y. Ma, W. Yang, Ammonium-functionalized hollow polymer particles as a pH-responsive adsorbent for selective removal of acid dye, ACS Appl. Mater. Interfaces 8 (26) (Jul. 2016) 16690–16698, https://doi.org/10.1021/ACSAMI.6B04199/SUPPL_FILE/AM6B04199_SI_001.PDF.
[113] Y. Wang, W. Wang, A. Wang, Efficient adsorption of methylene blue on an alginate-based nanocomposite hydrogel enhanced by organo-illite/smectite clay, Chem. Eng. J. 228 (Jul. 2013) 132–139, https://doi.org/10.1016/J.CEJ.2013.04.090.
[114] T. Lu, et al., Post-crosslinking towards stimuli-responsive sodium alginate beads for the removal of dye and heavy metals, Carbohydr. Polym. 133 (Nov. 2015) 587–595, https://doi.org/10.1016/J.CARBPOL.2015.07.048.
[115] K.T. Kubra, M.S. Salman, M.N. Hasan, Enhanced toxic dye removal from wastewater using biodegradable polymeric natural adsorbent, J. Mol. Liq. 328 (Apr. 2021) 115468, https://doi.org/10.1016/J.MOLLIQ.2021.115468.
[116] Q. Lin, M. Gao, J. Chang, H. Ma, Adsorption properties of crosslinking carboxymethyl cellulose grafting dimethyldiallylammonium chloride for cationic and anionic dyes, Carbohydr. Polym. 151 (Oct. 2016) 283–294, https://doi.org/10.1016/J.CARBPOL.2016.05.064.
[117] X. Qi, L. Wu, T. Su, J. Zhang, W. Dong, Polysaccharide-based cationic hydrogels for dye adsorption, Colloids Surf. B Biointerfaces 170 (Oct. 2018) 364–372, https://doi.org/10.1016/J.COLSURFB.2018.06.036.
[118] K. Bello, B.K. Sarojini, B. Narayana, A. Rao, K. Byrappa, A study on adsorption behavior of newly synthesized banana pseudo-stem derived superabsorbent hydrogels for cationic and anionic dye removal from effluents, Carbohydr. Polym. 181 (Feb. 2018) 605–615, https://doi.org/10.1016/J.CARBPOL.2017.11.106.
[119] S. Thakur, O.A. Arotiba, Synthesis, swelling and adsorption studies of a pH-responsive sodium alginate–poly(acrylic acid) superabsorbent hydrogel, Polym. Bull. 75 (10) (Oct. 2018) 4587–4606, https://doi.org/10.1007/S00289-018-2287-0/METRICS.
[120] S. Pandey, J.Y. Do, J. Kim, M. Kang, Fast and highly efficient removal of dye from aqueous solution using natural locust bean gum based hydrogels as adsorbent, Int. J. Biol. Macromol. 143 (Jan. 2020) 60–75, https://doi.org/10.1016/J.IJBIOMAC.2019.12.002.
[121] A. Salama, N. Shukry, M. El-Sakhawy, Carboxymethyl cellulose-g-poly(2-(dimethylamino) ethyl methacrylate) hydrogel as adsorbent for dye removal, Int. J. Biol. Macromol. 73 (1) (Feb. 2015) 72–75, https://doi.org/10.1016/J.IJBIOMAC.2014.11.002.
[122] G. Li, J. Ye, Q. Fang, F. Liu, Amide-based covalent organic frameworks materials for efficient and recyclable removal of heavy metal lead (II), Chem. Eng. J. 370 (Aug. 2019) 822–830, https://doi.org/10.1016/J.CEJ.2019.03.260.
[123] A. Shahat, M.R. Awual, M. Naushad, Functional ligand anchored nanomaterial based facial adsorbent for cobalt(II) detection and removal from water samples, Chem. Eng. J. 271 (Jul. 2015) 155–163, https://doi.org/10.1016/J.CEJ.2015.02.097.
[124] M.R. Awual, M.M. Hasan, Colorimetric detection and removal of copper(II) ions from wastewater samples using tailor-made composite adsorbent, Sens Actuators B Chem 206 (Jan. 2015) 692–700, https://doi.org/10.1016/J.SNB.2014.09.086.
[125] M. D'Halluin, J. Rull-Barrull, G. Bretel, C. Labrugère, E. Le Grognec, F.X. Felpin, Chemically modified cellulose filter paper for heavy metal remediation in water, ACS Sustain Chem Eng 5 (2) (Feb. 2017) 1965–1973, https://doi.org/10.1021/ACSSUSCHEMENG.6B02768/ASSET/IMAGES/MEDIUM/SC-2016-02768Q_0013.GIF.
[126] Q. Liu, et al., Superior adsorption capacity of functionalised straw adsorbent for dyes and heavy-metal ions, J. Hazard. Mater. 382 (Jan. 2020) 121040, https://doi.org/10.1016/J.JHAZMAT.2019.121040.
[127] C. Zhang, et al., Titanium dioxide/magnetic metal-organic framework preparation for organic pollutants removal from water under visible light, Colloids Surf. A Physicochem. Eng. Asp. 589 (Feb. 2020) 124484, https://doi.org/10.1016/J.COLSURFA.2020.124484.
[128] J. Yu, T. Wang, S. Rtimi, Magnetically separable TiO2/FeOx/POM accelerating the photocatalytic removal of the emerging endocrine disruptor: 2,4-dichlorophenol, Appl Catal B 254 (Oct. 2019) 66–75, https://doi.org/10.1016/J.APCATB.2019.04.088.
[129] M. Rafieezadeh, A.H. Kianfar, Fabrication of heterojunction ternary Fe3O4/TiO2/CoMoO4 as a magnetic photocatalyst for organic dyes degradation under sunlight irradiation, J Photochem Photobiol A Chem 423 (Jan. 2022) 113596, https://doi.org/10.1016/J.JPHOTOCHEM.2021.113596.
[130] S. Zhan, et al., Synthesis, characterization and dye removal behavior of core–shell–shell Fe3O4/Ag/polyoxometalates ternary nanocomposites, Nanomaterials 9 (9) (Sep. 2019) 1255, https://doi.org/10.3390/NANO9091255, 2019, Vol. 9, Page 1255.
[131] P.F. Wu, Q. Xue, T.Y. Wang, S.J. Li, G.P. Li, G.L. Xue, A PW12/Ag functionalized mesoporous silica-coated magnetic Fe3O4 core–shell composite as an efficient and recyclable photocatalyst, Dalton Trans. 50 (2) (Jan. 2021) 578–586, https://doi.org/10.1039/D0DT03882B.
[132] S.H. Ammar, A. Ibrahim Elaibi, I.Sh. Mohammed, Core/shell Fe3O4@Al2O3-PMo magnetic nanocatalyst for photocatalytic degradation of organic pollutants in an internal loop airlift reactor, Journal of Water Process Engineering 37 (Oct. 2020) 101240, https://doi.org/10.1016/J.JWPE.2020.101240.
[133] S.H. Ammar, W.A. Abdulnabi, H.D.A. Kader, Synthesis, characterization and environmental remediation applications of polyoxometalates-based magnetic zinc oxide nanocomposites (Fe3O4@ZnO/PMOs), Environ Nanotechnol Monit Manag 13 (May 2020) 100289, https://doi.org/10.1016/J.ENMM.2020.100289.
[134] X. Li, J. He, W. Zhang, L. You, J. Li, Ag nanoparticles interlayered Fe3O4/Ag/m(TiO2-ZrO2) magnetic photocatalysts with enhanced stability and photocatalytic performance for Cr(VI) reduction, Appl. Surf. Sci. 607 (Jan. 2023) 155076, https://doi.org/10.1016/J.APSUSC.2022.155076.
[135] J. He, Z. Zheng, I.M.C. Lo, Different responses of gram-negative and gram-positive bacteria to photocatalytic disinfection using solar-light-driven magnetic TiO2-based material, and disinfection of real sewage, Water Res. 207 (Dec. 2021) 117816, https://doi.org/10.1016/J.WATRES.2021.117816.
[136] E.M. Khudhair, S.H. Ammar, H.J. Khadim, Phosphotungstic acid immobilized onto ZnO coated zerovalent iron (Fe@ZnO/PW) core/shell magnetic nanocomposite for enhanced photocatalytic bacterial inactivation under visible light, J Photochem Photobiol A Chem 404 (Jan. 2021) 112907, https://doi.org/10.1016/J.JPHOTOCHEM.2020.112907.
[137] M. Nadimi, A. Ziarati Saravani, M.A. Aroon, A. Ebrahimian Pirbazari, Photodegradation of methylene blue by a ternary magnetic TiO2/Fe3O4/graphene oxide nanocomposite under visible light, Mater. Chem. Phys. 225 (Mar. 2019) 464–474, https://doi.org/10.1016/J.MATCHEMPHYS.2018.11.029.
[138] G. Yao, W. Bi, H. Liu, pH-responsive magnetic graphene oxide/poly(NVI-co-AA) hydrogel as an easily recyclable adsorbent for cationic and anionic dyes, Colloids Surf. A Physicochem. Eng. Asp. 588 (Mar. 2020) 124393, https://doi.org/10.1016/J.COLSURFA.2019.124393.
[139] F. Ghorbani, S. Kamari, Core–shell magnetic nanocomposite of Fe3O4@SiO2@NH2 as an efficient and highly recyclable adsorbent of methyl red dye from aqueous environments, Environ. Technol. Innov. 14 (May 2019) 100333, https://doi.org/10.1016/J.ETI.2019.100333.
[140] N.N.A. Malek, A.H. Jawad, K. Ismail, R. Razuan, Z.A. Alothman, Fly ash modified magnetic chitosan-polyvinyl alcohol blend for reactive orange 16 dye removal: adsorption parametric optimization, Int. J. Biol. Macromol. 189 (Oct. 2021) 464–476, https://doi.org/10.1016/J.IJBIOMAC.2021.08.160.
[141] C. Santhosh, et al., Synthesis and characterization of magnetic biochar adsorbents for the removal of Cr(VI) and acid orange 7 dye from aqueous solution, Environ. Sci. Pollut. Res. 27 (26) (Sep. 2020) 32874–32887, https://doi.org/10.1007/S11356-020-09275-1/TABLES/5.
[142] Q.U. Ain, M.U. Farooq, M.I. Jalees, Application of magnetic graphene oxide for water purification: heavy metals removal and disinfection, Journal of Water Process Engineering 33 (Feb. 2020) 101044, https://doi.org/10.1016/J.JWPE.2019.101044.
[143] X. Zhou, C. Jin, G. Liu, G. Wu, S. Huo, Z. Kong, Functionalized lignin-based magnetic adsorbents with tunable structure for the efficient and selective removal of Pb(II) from aqueous solution, Chem. Eng. J. 420 (Sep. 2021) 130409, https://doi.org/10.1016/J.CEJ.2021.130409.
[144] H. Hinsene, N. Bhawawet, A. Imyim, Rice husk biochar doped with deep eutectic solvent and Fe3O4/ZnO nanoparticles for heavy metal and diclofenac removal from water, Sep. Purif. Technol. 339 (Jul. 2024) 126638, https://doi.org/10.1016/J.SEPPUR.2024.126638.
[145] C.M. Chabib, J.K. Ali, M.A. Jaoude, E. Alhseinat, I.A. Adeyemi, I.M. Al Nashef, Application of deep eutectic solvents in water treatment processes: a review, Journal of Water Process Engineering 47 (Jun. 2022) 102663, https://doi.org/10.1016/J.JWPE.2022.102663.
[146] A. Zhou, et al., Comparative adsorption of emerging contaminants in water by functional designed magnetic poly(N-isopropylacrylamide)/chitosan hydrogels, Sci. Total Environ. 671 (Jun. 2019) 377–387, https://doi.org/10.1016/J.SCITOTENV.2019.03.183.
[147] Q. Zhou, et al., Magnetic and thermal dual-sensitive core-shell nanoparticles for highly preconcentration and measurement of Sudan red pollutants, Chemosphere 279 (Sep. 2021) 130584, https://doi.org/10.1016/J.CHEMOSPHERE.2021.130584.
[148] H. Tomonaga, Y. Tanigaki, K. Hayashi, T. Matsuyama, J. Ida, Adsorption properties of poly(NIPAM-co-AA) immobilized on silica-coated magnetite nanoparticles prepared with different acrylic acid content for various heavy metal ions, Chem. Eng. Res. Des. 171 (Jul. 2021) 213–224, https://doi.org/10.1016/J.CHERD.2021.05.005.
[149] J.J. Chen, A.L. Ahmad, J.K. Lim, B.S. Ooi, Adsorption-desorption characteristic of thermo-magneto-responsive poly(N-isopropylacrylamide)-co-acrylic acid composite hydrogel towards chromium (III) ions, Journal of Water Process Engineering 32 (Dec. 2019) 100957, https://doi.org/10.1016/J.JWPE.2019.100957.
[150] H. Zheng, et al., Tailor-made magnetic nanocomposite with pH and thermo-dual responsive copolymer brush for bacterial separation, Food Chem. 358 (Oct. 2021) 129907, https://doi.org/10.1016/J.FOODCHEM.2021.129907.
[151] Q. Zhou, et al., Magnetic solid phase extraction of bisphenol A, phenol and hydroquinone from water samples by magnetic and thermo dual-responsive core-shell nanomaterial, Chemosphere 238 (Jan. 2020) 124621, https://doi.org/10.1016/J.CHEMOSPHERE.2019.124621.
[152] C. Liu, Y. Li, Q. Duan, Preparation of magnetic and thermal dual-responsive zinc-tetracarboxyl-phthalocyanine-g-Fe3O4@SiO2@TiO2-g-poly(N-isopropyl acrylamide) core-shell green photocatalyst, Appl. Surf. Sci. 503 (Feb. 2020) 144111, https://doi.org/10.1016/J.APSUSC.2019.144111.
[153] J. Wang, M. Sgarzi, Z. Němečková, J. Henych, N. Licciardello, G. Cuniberti, Reusable and antibacterial polymer-based nanocomposites for the adsorption of dyes and the visible-light-driven photocatalytic degradation of antibiotics, Global Chall. 6 (11) (Nov. 2022) 2200076, https://doi.org/10.1002/GCH2.202200076.
[154] L.Y. Yee, et al., A novel tri-functionality pH-magnetic-photocatalytic hybrid organic-inorganic polyoxometalates augmented microspheres for polluted water

treatment, Membranes 13 (2) (Jan. 2023) 174, https://doi.org/10.3390/MEMBRANES13020174, 2023, Vol. 13, Page 174.